

Petrology and geochemistry of igneous inclusions in recent Merapi deposits: a window into the sub-volcanic plumbing system

J. P. Chadwick · V. R. Troll · T. E. Waight ·
F. M. van der Zwan · L. M. Schwarzkopf

Received: 19 April 2012 / Accepted: 30 August 2012 / Published online: 26 September 2012
© Springer-Verlag 2012

Abstract Recent basaltic-andesite lavas from Merapi volcano contain abundant and varied igneous inclusions suggesting a complex sub-volcanic magmatic system for Merapi volcano. In order to better understand the processes occurring beneath Merapi, we have studied this suite of inclusions by petrography, geochemistry and geobarometric calculations. The inclusions may be classified into four main suites: (1) highly crystalline basaltic-andesite

inclusions, (2) co-magmatic enclaves, (3) plutonic crystalline inclusions and (4) amphibole megacrysts. Highly crystalline basaltic-andesite inclusions and co-magmatic enclaves typically display liquid–liquid relationships with their host rocks, indicating mixing and mingling of distinct magmas. Co-magmatic enclaves are basaltic in composition and occasionally display chilled margins, whereas highly crystalline basaltic-andesite inclusions usually lack chilling. Plutonic inclusions have variable grain sizes and occasionally possess crystal layering with a spectrum of compositions spanning from gabbro to diorite. Plagioclase, pyroxene and amphibole are the dominant phases present in both the inclusions and the host lavas. Mineral compositions of the inclusions largely overlap with compositions of minerals in recent and historic basaltic-andesites and the enclaves they contain, indicating a cognate or ‘antelithic’ nature for most of the plutonic inclusions. Many of the plutonic inclusions plot together with the host basaltic-andesites along fractional crystallisation trends from parental basalt to andesite compositions. Results for mineral geobarometry on the inclusions suggest a crystallisation history for the plutonic inclusions and the recent and historic Merapi magmas that spans the full depth of the crust, indicating a multi-chamber magma system with high amounts of semi-molten crystalline mush. There, crystallisation, crystal accumulation, magma mixing and mafic recharge take place. Comparison of the barometric results with whole rock Sr, Nd, and Pb isotope data for the inclusions suggests input of crustal material as magma ascends from depth, with a significant late addition of sedimentary material from the uppermost crust. The type of multi-chamber plumbing system envisaged contains large portions of crystal mush and provides ample opportunity to recycle the magmatic crystalline roots as well as interact with the surrounding host lithologies.

Communicated by J.Hoefs.

Electronic supplementary material The online version of this article (doi:10.1007/s00410-012-0808-7) contains supplementary material, which is available to authorized users.

J. P. Chadwick · F. M. van der Zwan
Department of Petrology, Vrije Universiteit, De Boelelaan 1085,
1081 HV Amsterdam, The Netherlands

Present Address:

J. P. Chadwick
Science Gallery, Trinity College Dublin,
Pearse Street, Dublin, Ireland

V. R. Troll (✉)

Department of Earth Sciences, CEMPEG, Uppsala Universitet,
Villavägen 16, 75236 Uppsala, Sweden
e-mail: valentin.troll@geo.uu.se

T. E. Waight

Department of Geography and Geology, University of
Copenhagen, Øster Voldgade 10, 1350 Copenhagen, Denmark

Present Address:

F. M. van der Zwan
GEOMAR/Helmholtz Centre for Ocean Research Kiel,
Wischofstr. 1-3, 24148 Kiel, Germany

L. M. Schwarzkopf

GeoDocCon, Unterperfdt 8, 95176 Konradsreuth, Germany

Keywords Basaltic-andesite · Co-magmatic enclaves · Plutonic inclusion · Merapi plumbing system

Introduction

In subduction zone settings, primary mafic magma is generated in the mantle wedge (Davies and Stevenson 1992; Sisson and Bronto 1998). Modification of primary melts on ascent occurs by numerous processes, most importantly (fractional) crystallisation and crustal contamination, but is further modified by magma mixing and degassing (e.g. Bowen 1928; DePaolo 1981; Gill 1981; Grove and Kinzler 1986; Hildreth and Moorbath 1988; Rogers and Hawkesworth 1989; Davidson and Tepley 1997; Annen et al. 2006). Such processes can sometimes be identified in the resulting whole rock geochemistry of erupted magmas; however, the details of these processes are often difficult to discern (e.g. Chadwick et al. 2007; Price et al. 2007, 2010). Igneous inclusions and individual megacrysts hosted in lavas provide a means of investigating varied crystallisation environments and/or processes, as they may preserve distinct and subtle records of crystallisation during ascent (Grove et al. 1988; Renzulli and Santi 1997; Burt et al. 1998; Dungan and Davidson 2004). Crystalline plutonic inclusions in arc magmas have been identified in numerous studies as fractionation residues reflecting crustal solidification processes (e.g. Beard and Borgia 1989; Heliker 1995; Costa et al. 2002). Megacrysts may be high-pressure phases that can be related to their host magma (co-genetic), or incorporated fragments of older coarsely crystalline zones (i.e. antecrysts, Davidson et al. 2007) from over a range of pressure and temperature conditions that merely happen to erupt with the host lavas (e.g. Irving 1974; Irving and Frey 1984; Bodinier et al. 1987; Burt et al. 1998). Thus, co-eruptive igneous inclusions may preserve distinct records of magma differentiation processes and therefore complement host magma whole rock geochemistry.

Merapi volcano on Java, Indonesia, has been subjected to numerous studies in recent years (e.g. Newhall et al. 2000; Gertisser et al. 2012) in an effort to better understand the volcanic system and to reduce risk vulnerability. This is especially relevant given its proximity to the major population centre Yogyakarta (~3.5 million inhabitants), which is located ~25 km South of Merapi's summit. However, the physical and chemical characteristics of the magmatic system that feed the volcano remain incompletely understood. We have analysed an extensive suite of igneous inclusions in order to investigate the processes occurring beneath Merapi volcano in more detail. Petrography, geochemistry and geobarometric calculations were utilised to

assist in unravelling the petrogenetic history of recent Merapi basaltic-andesites and their inclusions and thus to gain insight into the architecture of the magmatic plumbing system feeding the volcano.

Geological setting

Merapi is a large Quaternary strato-volcano (2,930 m.a.s.l.) currently characterised by periods of active dome growth and intermittent explosive events. The Merapi complex is situated on the active volcanic front of the Sunda arc, which is the result of the northward subduction of the continuous Indo-Australian Plate beneath Eurasia (Hamilton 1979; Jarrard 1986; Simkin and Siebert 1994; Tregoning et al. 1994; Bird 2003). The active Holocene arc in East to Central Java is bound to the south by the Southern Mountains Zone, remnants of the earlier Eocene to Miocene volcanic arc, and to the north by the Kendeng and Rembang Zones (Smyth et al. 2005). The most northerly Rembang zone represents accreted crustal slivers joined up in the Cretaceous. The Kendeng Zone is the main Cenozoic depocentre for the region (Smyth et al. 2005), and is thought to contain between 8 (de Genevraye and Samuel 1972) and 11 km (Untung and Sato 1978) of sediment. This sediment overlies a basement of uncertain composition, generally considered as 'immature arc crust', which extends up to 25 km below the surface (van Bemmelen 1949; Curray et al. 1977; Hamilton 1979; Jarrard 1986). This type of basement is also thought to make up the crust in the area below and immediately to the south of Merapi. There, surface exposures comprise a sequence of Cenozoic marine limestones and marls and volcanoclastic sediments with individual units that are up to 2 km thick (van Bemmelen 1949).

Merapi (Fig. 1) is presently characterised by block-and-ash flows and explosive events (Andreastuti et al. 2000; Camus et al. 2000; Surono et al. 2012). However, the stratigraphic record for Merapi indicates that frequent large explosive eruptions (up to >VEI 4) have occurred regularly in the past, implying that the volcano may revert to a more explosive eruptive style in the future (Camus et al. 2000; Andreastuti et al. 2000; Newhall et al. 2000; Gertisser and Keller 2003b). This poses a significant hazard to the city of Yogyakarta, some 25 km to the south, as well as the densely populated lower slopes of the volcano (Siswawidjono et al. 1995; Andreastuti et al. 2000; Camus et al. 2000; Itoh et al. 2000; Newhall et al. 2000; Thouret et al. 2000; Voight et al. 2000; Gertisser et al. 2011).

Merapi dome growth is typically associated with both deep and shallow earthquakes (volcano-tectonic and multi-phase (hybrid) seismic events, e.g., Ratdomopurbo and Poupinet 2000). Eruptions associated with deep volcano-tectonic (VT) earthquakes are believed to indicate magma

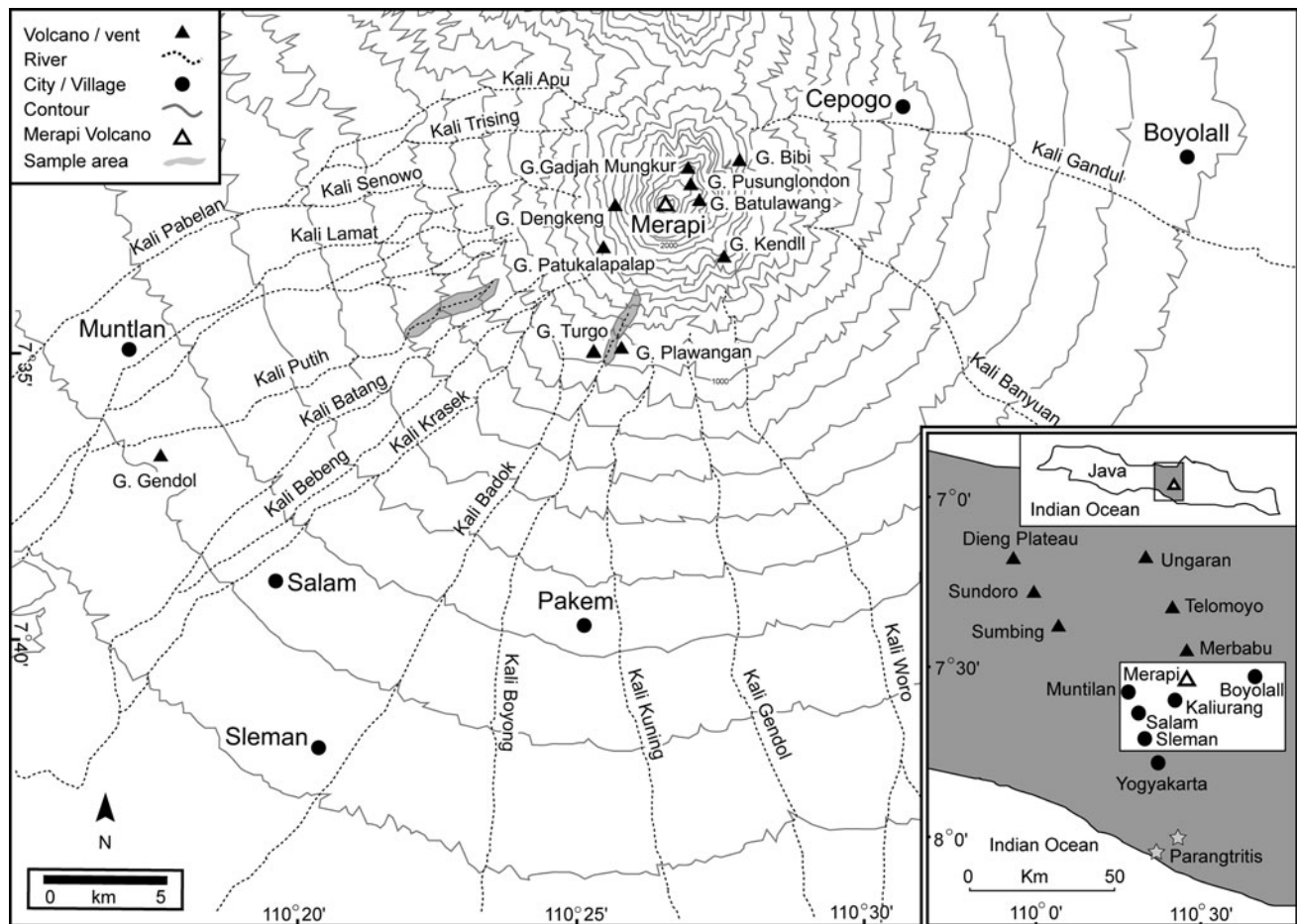


Fig. 1 A sketch map of the summit of Merapi (after Chadwick et al. 2007) with *inset* showing the location of Merapi relative to other Quaternary volcanoes in the region (*triangles*) and to areas of significant population (*filled circles*) in Central Java (after Gertisser

and Keller 2003b). Sampling location for Merapi deposits at Kali Putih (1998 deposits) and Kali Boyong (1994 deposits) are highlighted in *grey*

migration from a lower crustal magma reservoir (Ratdomopurbo and Poupinet 2000). In contrast, numerous pyroclastic eruptions at Merapi are associated with shallow hybrid seismic events and tremors (Hidayat et al. 2000; Ratdomopurbo and Poupinet 2000) which may indicate that a set of shallow processes act as eruption triggers in the higher levels of the volcanic plumbing system (cf. Ratdomopurbo and Poupinet 2000; Deegan et al. 2011). The identification of an aseismic zone at a depth of approximately 1.5–2.5 km below the summit in 1995 was taken to indicate the existence of a shallow magma storage system beneath Merapi (Ratdomopurbo and Poupinet 2000). While high-resolution gravity data have identified a high-density body beneath the summit of Mt. Merapi, (Tiede et al. 2005), GPS, tilt and seismic data (Westerhaus et al. 1998; Wassermann et al. 1998; Beauducel and Cornet 1999) do not provide evidence for a large, edifice-hosted, (i.e. shallow) magma reservoir. Furthermore, although a number of geophysical studies have looked at the internal structure of the Merapi edifice (e.g. Maercklin et al. 2000; Wegler and Lühr 2001; Müller et al. 2002; Müller and Haak

2004), no conclusive evidence for a continuous edifice-hosted chamber has been suggested. Geochemical data do, in turn, suggest a quasi-steady state magma supply system beneath Merapi (Gertisser 2001; Gertisser and Keller 2003b). Moreover, recent tomographic work has identified a large tomographic anomaly in the crust and upper mantle beneath Merapi that seems to extend all the way to the subducting slab (Koulakov et al. 2007; Wagner et al. 2007), indicating that the magma supply system beneath the volcano is potentially far more extensive than previously thought.

Recent Merapi volcanics exhibit a high-K basaltic-andesite composition and a relatively restricted spread in whole rock and isotope geochemistry (Bahar 1984; del Marmol 1989; Hammer et al. 2000; Gertisser and Keller 2003a). However, intra-crystalline Sr isotope variation and the presence of numerous inclusions of both igneous and meta-sedimentary origin in recent deposits suggest the operation of a whole spectrum of additional magmatic processes are at play (e.g. Chadwick et al. 2007; Deegan et al. 2010; Gertisser et al. 2011; Troll et al. 2012a). In

addition, plagioclase crystals display complex textures, such as (reverse) zoning and dissolution features (e.g. sieve-textured rims), indicative of a long and complex magmatic history (e.g. Chadwick et al. 2007). In a large and long-lived system such as Merapi, intra-crustal magma differentiation processes are likely to be significant in magmatic evolution and their identification and localisation is integral to understanding the dynamics of the volcano.

Terminology

The terminology we used to describe the inclusions present in recent Merapi deposits is defined as follows. ‘Highly crystalline basaltic-andesite inclusions’ refer to samples that show similar mineralogy to the host magmas, but with a greater abundance of crystals of mainly plagioclase. These often occur as schlieren and domains in the host lavas. The term ‘co-magmatic enclaves’ is used to refer to basaltic igneous inclusions that display liquid and/or chilled crenulated and lobate contacts with the host magma. Enclaves and basaltic-andesite schlieren are co-magmatic in the sense that both host and inclusion were liquid magma simultaneously. ‘Amphibole megacryst’ refers to, in our case, amphibole crystals of >10 mm in size (but can range up to several cm across), they appear not to be in equilibrium with the host basaltic-andesite based on textural observations. ‘Plutonic crystalline inclusions’ refer to predominantly medium- to coarsely crystalline inclusions of igneous fragments encased within Merapi lavas. These plutonic inclusions may represent: (a) a coarsely crystalline portion of currently erupting magma, that is, co-magmatic; (b) material genetically related to the erupting magma, but a precursor to current eruptive products, that is, crystalline fragments of an earlier magma batch (cognate or ‘antelithic’); or (c) material that is genetically unrelated to the magmatic system, that is, xenolithic (*sensu lato*). Plutonic crystalline inclusions may contain up to 10 % vesiculated glass and finely crystalline groundmass. Lithological nomenclature of the plutonic inclusions is after Streckeisen (1976) and Le Maitre (1989). The term ‘felsic’ is loosely used to refer to inclusions that are mineralogically dominated by feldspar and the term ‘mafic’ is employed to refer to inclusions that are mineralogically dominated by pyroxene and/or amphibole.

Samples and analytical methods

Inclusions of both igneous and meta-sedimentary compositions were identified in the 1994 and the 1998 block-and ash-flow deposits and collected in September 1999 and March/April 2002, from Kali (valley in Indonesian) Boyong and Jurangero quarry at Kali Putih, respectively

(Fig. 1). The inclusions comprise only a small percentage of the total deposits that are estimated to be approximately 2.5–3 km³ for the 1994 event (Abdurachman et al. 2000) and approximately 2.5–4.3 km³ for the 1998 event (Schwarzkopf et al. 2005). The block-and-ash flow deposits are comprised of three components: a basal avalanche, a low-density ground surge, and an ash layer (Schwarzkopf et al. 2005). The basaltic-andesite and inclusion samples analysed in this study are typically clasts from poorly sorted basal avalanche deposits. Decimetre- to centimetre-sized basaltic-andesite blocks are set in a fine ash matrix, with the largest blocks in the deposits typically between 1 and 3 m in size, but rare exceptions of blocks that are up to 20 m across. The enclaves, plutonic crystalline inclusions and megacrysts are usually encased in host basaltic-andesite blocks, but the plutonic fragments do sometimes form clasts by themselves.

Seventeen plutonic crystalline inclusions, four co-magmatic enclaves, one highly crystalline basaltic-andesite inclusion, four basaltic-andesites, seven calc-silicate xenoliths and four volcanoclastic xenoliths (supplementary Table 1) were prepared for whole rock major element analysis. Trace elements were measured for all plutonic crystalline inclusions and co-magmatic enclaves and for two of the calc-silicate xenoliths and three of the volcanoclastic xenoliths. Isotope analysis was performed on a selection of eight plutonic inclusions, two basaltic enclaves, three calc-silicate xenoliths and three volcanoclastic xenoliths. Preparation of the rocks was done by carefully removing weathered surfaces and cutting pristine blocks for crushing. The blocks were crushed with a hammer and the resulting chips were washed and hand-picked to eliminate weathered fragments. Samples were then powdered using an agate ball mill.

Major and trace element concentrations of selected samples were determined by X-Ray Fluorescence spectrometry (XRF) analysis of fused glass beads at GEOMAR in Kiel, Germany, using an automated Phillips PW1480 X-ray spectrometer. All analyses were carried out with a Rh X-ray tube and calibrated to international geological reference standards BHVO-1, JA-2, JB-2, JB-3 and JR-1; standard analyses are reported by Abratis et al. (2002). Rare earth elements (REE) were analysed by inductively coupled plasma mass spectrometry (ICP-MS) at the Rock Geochemical Laboratory of the Geological Survey of Denmark and Greenland (GEUS) in Copenhagen, Denmark. The samples were prepared following the method described by Turner et al. (1999) and were analysed using a Perkin-Elmer[®] 6100 DRC Quadrupole ICP-MS with a Meinhard nebulizer. Detection limits and analytical precision range from <100 ppb to <1 ppt, and relative analytical precision is typically ~2–5 % (one standard deviation).

Major element mineral analyses were carried out on Amph, Px and Pl in polished and carbon-coated thin sections of 7 selected plutonic crystalline inclusions, 3 comagmatic enclaves and 1 amphibole megacryst, using the JEOL JXA-8200 Superprobe at the Department of Geography and Geology, University of Copenhagen. Analysis locations were selected using backscatter electron images, allowing positioning accurate to approximately 1 μm . Samples were analysed for Si, Ti, Al, Fe, Mg, Ca, Na, K, Mn, Cr and Ni. In order to minimise Na-loss, this element was analysed at the beginning of the sequence. Na counts were monitored during analysis and remained stable over the measurement time. An electron beam of 2 μm in diameter and a current of 15–30 nA was used with a count time of 30 s off peak and 30 s on peak. Relative analytical precision was <1 % for Si, Al and Ca, 2–3 % for Na, <10 % for Fe and K and 20 % for Mg and Ti.

Selected whole rock samples were analysed for Sr, Nd and Pb isotopes. Approximately 200 mg of sample was leached with HCl to remove alteration and then dissolved using conventional HF–HCl–HNO₃ dissolution techniques in Teflon beakers. Sr and Nd were separated using standard ion exchange column chemistry (see Waight et al. 2002). Sr isotopes were measured by thermal ionisation mass spectrometry (TIMS) at Department of Geography and Geology in Copenhagen using a VG Sector 54-IT employing the methods outlined in Pietranik and Waight (2008). Nd and Pb were analysed using a VG Axiom multiple collector inductively coupled plasma mass spectrometer (MC-ICPMS) at the Danish Lithosphere Centre in Copenhagen following the methodology outlined in Luais et al. (1997) for Nd isotope analyses and the double spike method of Baker et al. (2004) for high-precision Pb isotope measurements. Over the period of analyses, replicate

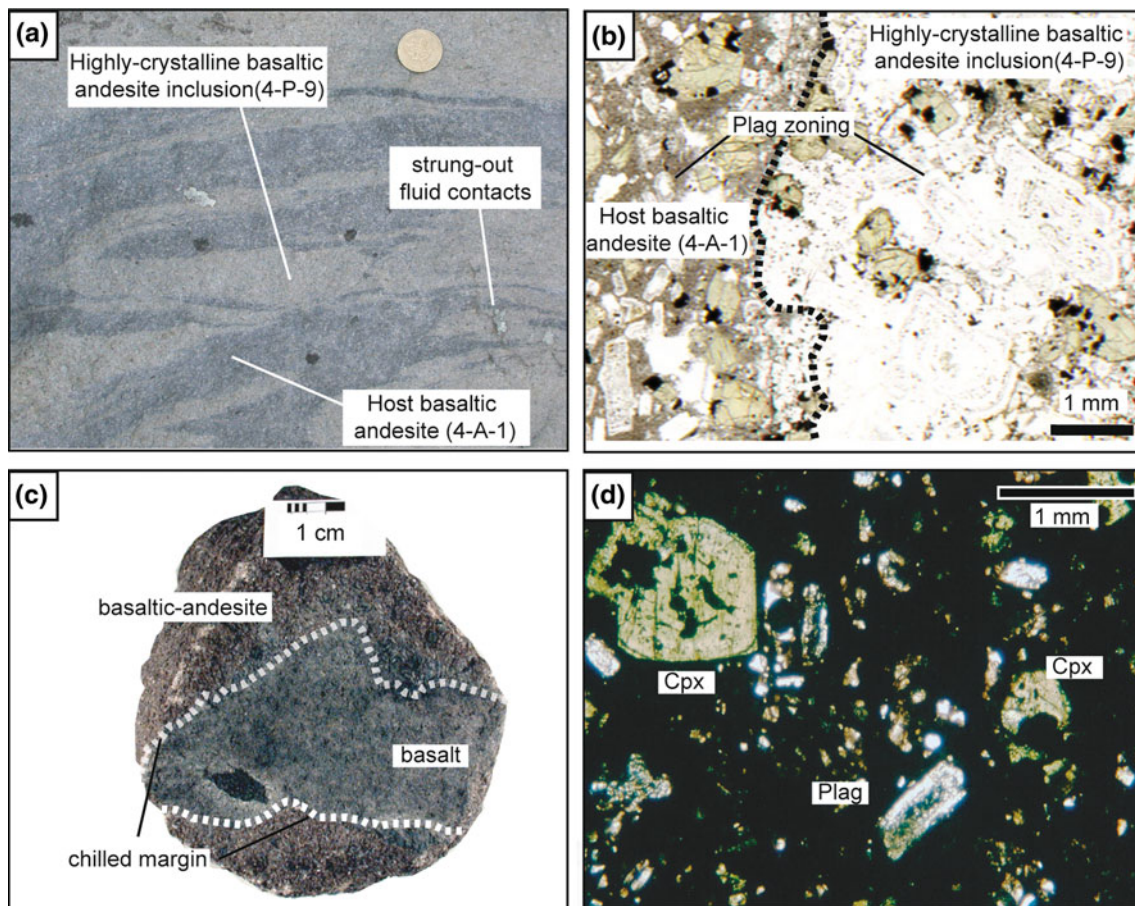
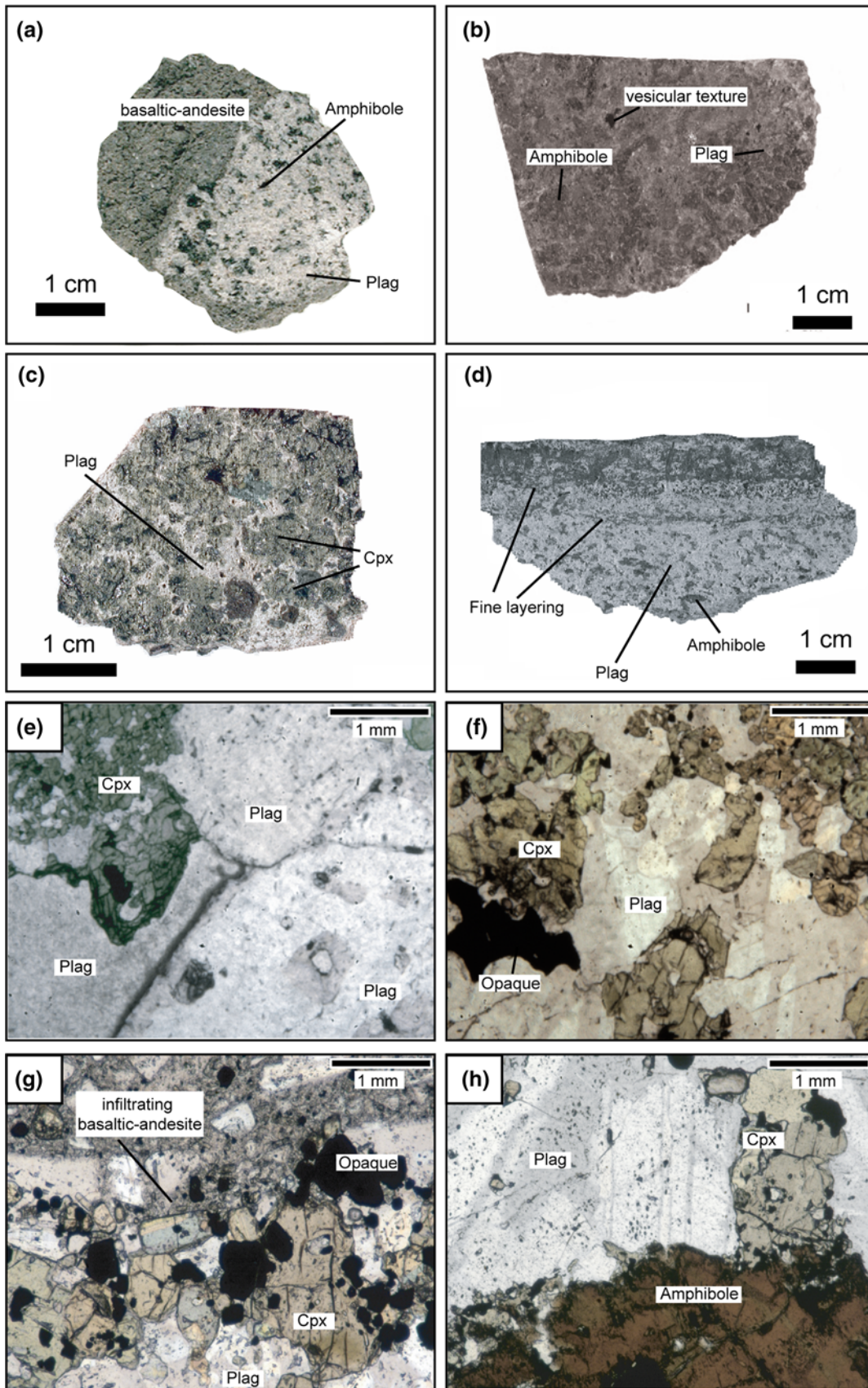


Fig. 2 **a** Field photograph of basaltic-andesite mixing textures in outcrop, with coin for scale. Darker basaltic-andesite (4-A-1) has strung out lenticular shapes indicating fluid–fluid relationships with the lighter highly crystalline basaltic-andesite inclusions (4-P-9). **b** Typical photomicrograph of highly crystalline basaltic-andesite inclusion in a host basaltic-andesite lava. Though the crystallinity is variable between the two, both display dominantly zoned plagioclase,

with lesser clinopyroxene (cpx) and opaques. **c** Hand sample of a basaltic enclave (8-B-1) in basaltic-andesite with a chilled fluid contact with its host rock. White dashed lines highlight the margin of the basalt enclave. **d** Photomicrograph of a thick section (150 mm) of a basaltic enclave in XPL. The enclaves contain significantly less plagioclase, and generally smaller crystal sizes than the highly porphyritic basaltic-andesite host rock



◀ **Fig. 3** **a** Felsic plutonic inclusion that is coarsely crystalline and plagioclase rich. **b** Example of an amphibole-rich mafic plutonic inclusion (4-P-4) containing vesiculated glass. **c** Cpx rich mafic plutonic inclusion 8-P-12 also contains vesiculated glass. **d** Layered felsic plutonic inclusion 4-P-5 has alternating plagioclase-rich and amphibole-rich bands and alignment of long axes of crystals parallel to the layering. **e** Plane polarised light (PPL) image of triple junction between three plagioclase crystals and a heavily resorbed clinopyroxene crystal engulfed in a plagioclase poikiloblast (8-P-1). **f** PPL image of a felsic plutonic inclusion with closely interlocking texture between plagioclase and clinopyroxene with an irregularly shaped opaque crystal (8-P-4). **g** PPL image of sharp contact between a pyroxene gabbro and its host basaltic-andesite with infiltrating basaltic-andesite but no chilled margin (8-P-12). **h** PPL image of a large amphibole crystal with a reaction rim of opaques (8-P-10)

analyses of standards were as follows: SRM987 yielded $^{87}\text{Sr}/^{86}\text{Sr} = 0.710223 \pm 3$; DLC in-house mixed Ames Nd–Sm metal gave $^{143}\text{Nd}/^{144}\text{Nd} = 0.51211 \pm 7$ ($n = 9$); SRM 981 yielded $^{206}\text{Pb}/^{204}\text{Pb} = 16.9418 \pm 10$, $^{207}\text{Pb}/^{204}\text{Pb} = 15.4990 \pm 11$ and $^{208}\text{Pb}/^{204}\text{Pb} = 36.7245 \pm 34$

($n = 14$) (all errors 2 SD). Total procedural blanks were <100 pg for Sr, Nd and Pb and are insignificant compared to the amounts of material analysed.

Petrology of inclusions

The igneous inclusions contained in the 1994 and 1998 Merapi deposits are less abundant than the calc-silicate xenoliths previously described by Chadwick et al. (2007) and Troll et al. (2012a) and make up considerably less than 0.5 % of Merapi deposits. They can be divided into four main groups: (1) Highly crystalline basaltic-andesite inclusions (HCBA inclusions) (Fig. 2a, b), (2) co-magmatic enclaves (Fig. 2c, d), (3) plutonic crystalline inclusions (Fig. 3), and (4) amphibole megacrysts (Fig. 4). Mineral names, structural formulae and end-members were calculated using Leake et al. (1997) for amphibole and Morimoto (1988) for pyroxenes. Feldspar nomenclature follows Deer et al. (1992).

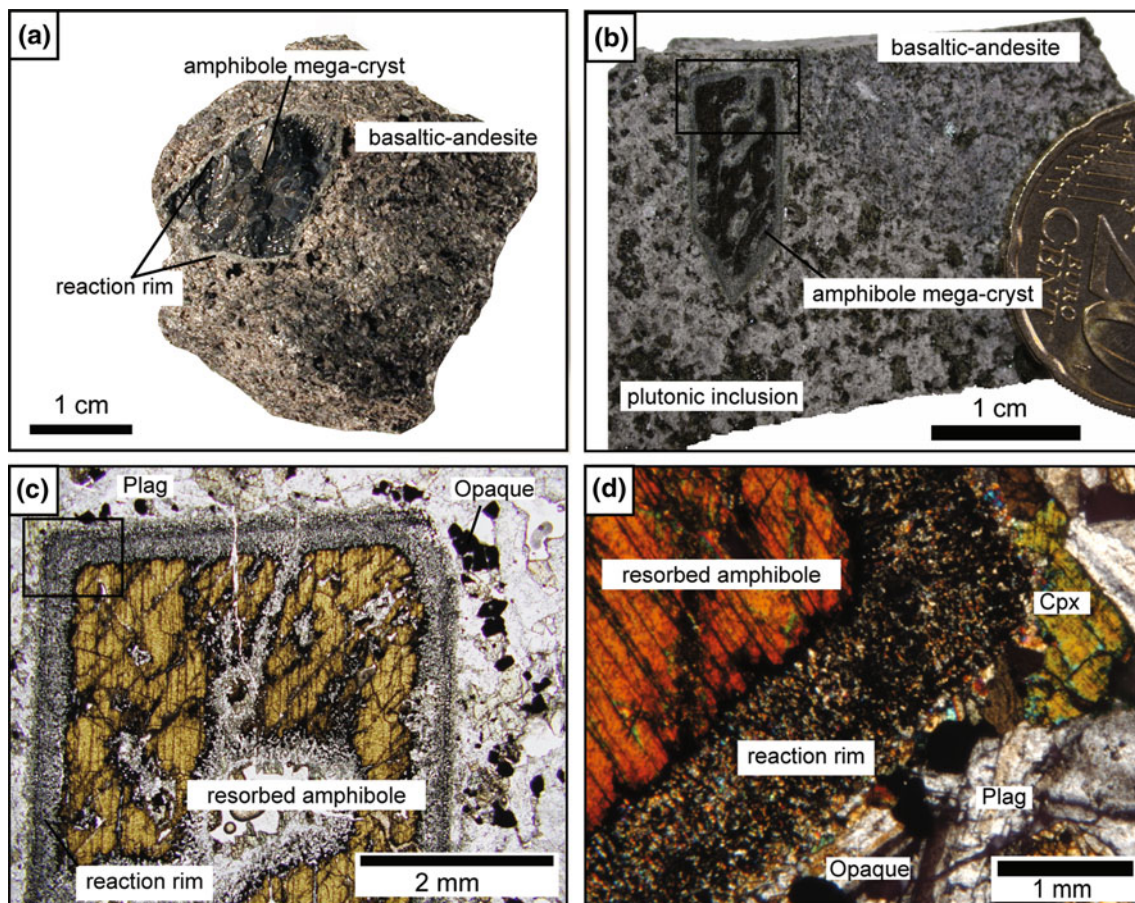


Fig. 4 **a** Amphibole megacryst with well developed reaction rim in hand sample, embedded in a host basaltic-andesite. **b** Hand sample of a plutonic inclusion (8-P-3) with a diffuse contact with its host basaltic-andesite. A small heavily resorbed amphibole megacryst with a well developed reaction rim traverses the contact. *Black box* denotes

area represented in (c). **c** Photomicrograph of resorbed amphibole megacryst in PPL. Area represented in (d) is denoted by the *black box*. **d** High magnification photomicrograph of amphibole megacryst in XPL showing the presence of plagioclase, clinopyroxene, and opaque phases in a granular reaction rim

Highly crystalline basaltic-andesite inclusions

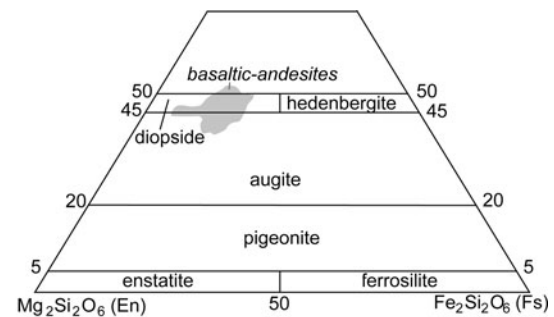
The HCBA inclusions are mineralogically and chemically very similar to the host basaltic-andesites and their plagioclase crystals have the same complex textures and zoning as those in the basaltic-andesites (Fig. 2a, b). However, they display a difference in texture due to their highly crystalline character. The inclusions consist of strung-out layers that display sharp contacts with intricate lobate margins and fluid–fluid relations in a host basaltic-andesite (schlieren), but lack chilled contacts with the host lavas (Fig. 2a); they are, however, less crystalline than the plutonic inclusions.

Co-magmatic basaltic enclaves

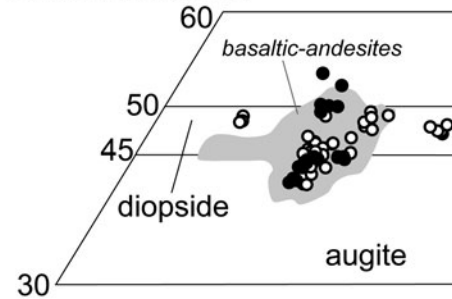
The basaltic enclaves are generally restricted in size to a few centimetres across (Fig. 2c). They typically possess elliptical shapes with lobate contacts with the host basaltic-andesite and frequently show distinct chilled margins (Fig. 2c). They are finely crystalline, with <1 mm phenocrysts of plagioclase and pyroxene set in a glassy to microcrystalline matrix, with mainly elongate to acicular plagioclase microcrysts (Fig. 2d). Clinopyroxenes are diopside to augite in composition ($Wo_{27-46}En_{27-44}Fs_{11-52}$) and range from subhedral to anhedral, with simple zoning frequently displayed. They plot within the range of compositions previously published for Merapi basaltic-andesite minerals (Gertisser 2001) (Fig. 5b). Hornblende is present in all samples and forms small laths with strong reaction rims. Plagioclase crystals also form relatively small elongate laths (Fig. 2d), which are normally zoned. The analysed plagioclase compositions in the magmatic enclaves have strongly bimodal population trends (Figs. 6, 7), with crystal rims and micro-crystals in the groundmass typically possessing compositions of andesine to labradorite An_{49-65} (average $An \sim 57$ and 54 for rims and groundmass respectively), while crystal cores have more calcic (bytownite) compositions of An_{70-90} , (average $An \sim 82$, $n = 15$) (Fig. 7). Representative mineral assemblages and analyses for these inclusions are presented in Tables 1 and 2.

Plutonic crystalline inclusions

The plutonic crystalline inclusions are typically 5–10 cm across, sub-rounded to angular, and may be subdivided based on modal mineralogy into relatively mafic amphibole- and clinopyroxene-gabbros and relatively felsic leucogabbros, anorthosites and diorites, although a continuous spectrum seems to be present (see Fig. 3; Table 1 for (representative) modal mineral abundances and textures). Contact with the host basaltic-andesite is typically sharp with alignment of phenocrysts in the host lava along



(a) Plutonic inclusions



(b) Co-magmatic enclaves

Fig. 5 Compositional ranges and nomenclature for Ca–Mg–Fe pyroxenes in plutonic inclusions and co-magmatic enclaves (after Morimoto 1988). Grey shaded area represents compositions for Merapi basaltic-andesites measured in this study with additional data from Gertisser 2001. **a** Pyroxene compositions from plutonic inclusions, black circles = mafic inclusions, white circles = felsic inclusions. **b** Pyroxene compositions from enclaves (grey diamonds). The plutonic inclusions, the enclaves and the host basaltic-andesites have overlapping pyroxene compositions

boundaries and often a concentration of oxides at the margin of the inclusions. There is no evidence for chilled domains in the host basaltic-andesite (Fig. 3a, g), indicating the plutonic inclusions were likely at a significant temperature upon incorporation into the host melt. The plutonic inclusions are typically medium to coarse grained and occasionally display asymmetric, millimetre to centimetre thick mineral layers indicative of crystal accumulation (e.g. Wager and Brown 1968; Campbell 1978) (Fig. 2d). Some of the inclusions possess up to 10 % vesiculated glass and some have a patchy micro-crystalline groundmass in a framework of plagioclase, pyroxene and

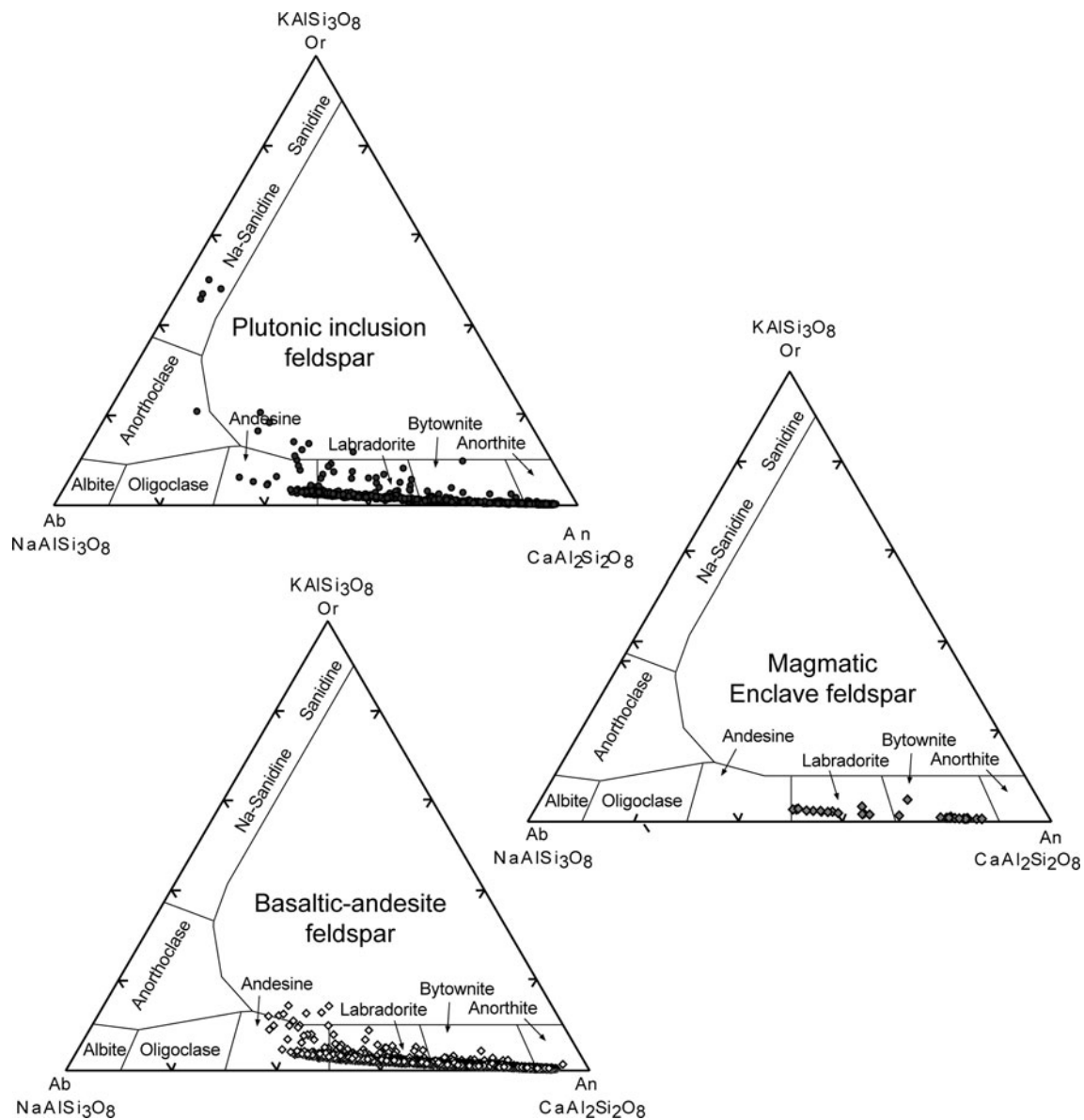


Fig. 6 Ternary feldspar nomenclature and composition diagrams for crystals in plutonic inclusions, enclaves and the host basaltic-andesite, indicating different but overlapping ranges in feldspar compositions for the different lithological groups

amphibole crystals. This groundmass may be primary and/or a late stage addition due to incorporation into Merapi host basaltic-andesite magma. Rounded vesicles in the glassy portions indicate that vesiculation was a late process. Crystals in rare samples, without groundmass or glass ($n = 2$), show sub-solidus textural re-equilibration along boundaries between plagioclase crystals and apparent dihedral angles of approximately 120° (cf. Hunter 1987; Fig. 3e, f), indicating these inclusions were crystalline upon incorporation into the host magma.

Mafic plutonic inclusions are mineralogically dominated by amphibole and/or pyroxene with oxides (titanomagnetite, spinel, ilmenite), lesser plagioclase and rare anhedral apatite and titanite as accessory phases between crystal

boundaries (Table 1). Plagioclase is the dominant phase in the felsic inclusions (Table 1) with lesser pyroxene, amphibole, oxides and accessory minerals present, including apatite and titanite. In both sub-groups, clinopyroxene of diopside to augite composition occurs, with an anhedral to subhedral crystal shapes, and occasionally normal zoning. Ca-rich clinopyroxene is present only in the mafic inclusions ($Wo_{41-56}En_{27-45}Fs_{7-24}$) (Fig. 5). Amphibole is commonly present as large laths >5 mm, which are dominantly magnesio-hastingsite with some pargasite and hornblende (cf. Leake et al. 1997). The amphibole laths often possess pronounced reaction rims populated by oxides and finely crystalline pyroxene, plagioclase and occasionally glass. Plagioclase crystals are typically

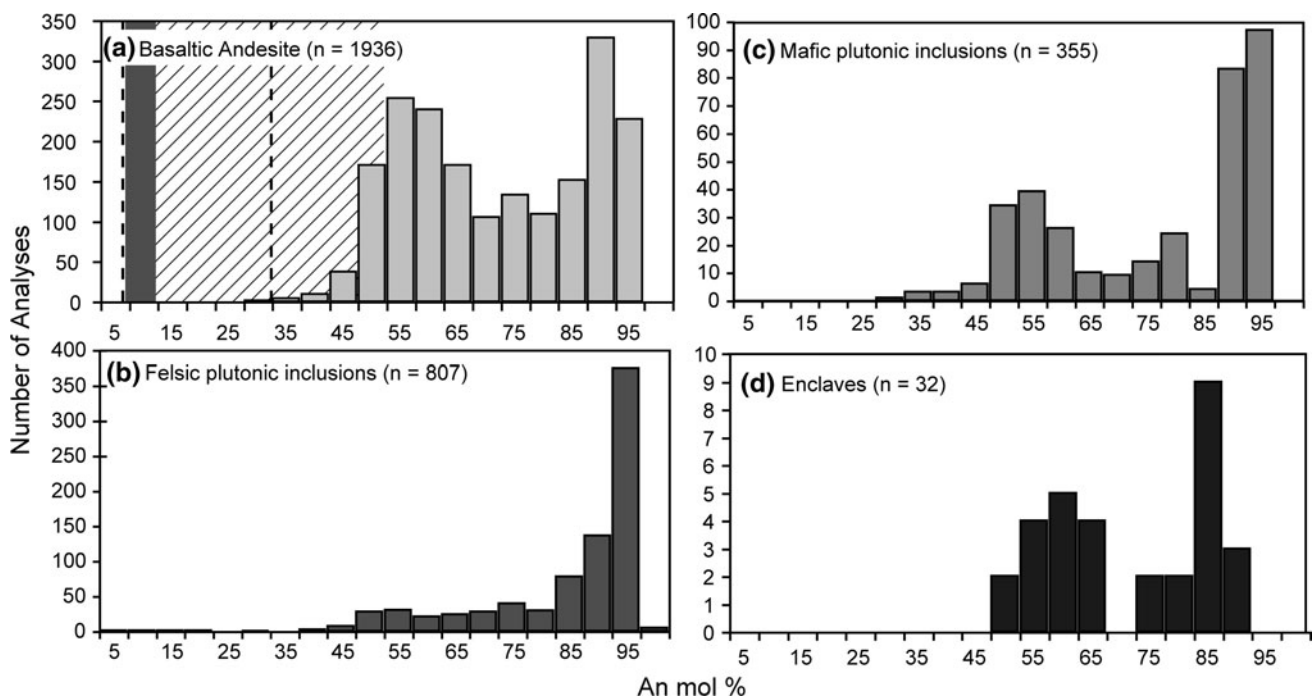


Fig. 7 Histograms of An mol % composition of analyses of feldspar from **a** host basaltic-andesite, **b** felsic plutonic inclusions, **c** mafic plutonic inclusions, and **d** co-magmatic enclaves. For comparison plagioclase groundmass compositions are given (between *dashed lines*), calculated according to CIPW norm based on representative

analyses of groundmass/glass compositions of Schwarzkopf et al. (2001) and Hammer et al. (2000), as well as microlite compositions from Hammer et al. (2000; *dashed band*: microlite core compositions; *dark grey band*: rim compositions)

concentrically zoned, subhedral and exhibit an unusually broad range in An mol % composition from 4 to 95 % (Fig. 6) with two dominant domains of An_{50–70} and An_{~90} (Fig. 6b, c, $n = 982$ total). The feldspar population in the felsic inclusions is unimodal, with mainly bytownite to anorthite present (Fig. 7b). The feldspar in the mafic inclusions is andesine to anorthite in composition (An_{30–95}), but displays a bimodal distribution, with most crystals having an An content of either 45–60 % or 85–95 % (Fig. 7c). Zoned crystals, 1–5 mm in size, are present; however, smaller crystals, <1 mm, are more commonly observed. Late feldspar in the groundmass and infilling cracks of both mafic and felsic inclusions are of a more restricted compositional range (An_{52–58}Ab_{41–52}Or_{2–3}). A limited number of analyses ($n = 5$, not included above) fall in the Na-sanidine to anorthoclase fields. These compositions appear to be the result of late alteration. Representative analyses for minerals in the plutonic inclusions are presented in Table 2.

Amphibole megacrysts

Amphibole megacrysts range in size from 0.5 cm up to 5 cm with rare samples up to 8 cm across (Fig. 4). One

heavily embayed and resorbed amphibole megacryst was also found within a felsic plutonic inclusion (8-P-3, Fig. 4). In thin section, the amphibole megacrysts are dark to reddish brown in colour, strongly pleochroic and often display perfect cleavage. All of the observed amphibole megacrysts are typically euhedral to subhedral with strong disequilibrium textures, including pronounced reaction rims and embayment textures (Fig. 4). These reaction rims are composed of fine-grained intergrowths of clinopyroxene, plagioclase and titanomagnetite and also occur along the cleavage planes of many large amphibole megacrysts. Glass is rare in the reaction rims of amphibole megacrysts, but observed in some smaller amphibole crystals that are likely to be phenocrysts (e.g. Gertisser et al. 2011). The replacement that occurs at the rims and along cleavage planes of several of the amphibole megacrysts (Fig. 4) is interpreted to be a late oxidation effect, but may also in part be decompression related (c.f. Garcia and Jacobson 1979; Devine et al. 1998; Rutherford and Devine 2003). The analysed amphibole megacrysts are magnesio-hastingsite to ferro-edenite (cf. Leake et al. 1997) and of similar compositions to amphibole observed in our mafic plutonic inclusions. Representative analyses of these inclusions are presented in Table 2.

Table 1 Mineralogy and textural features of representative igneous inclusions

Sample	Rock type	Average grain size ^a	Modal mineralogy (~ vol %)					Texture
			Cpx	Amph	Plag	Opaque	Glass/gm	
Felsic plutonic inclusions								
8-P-1	Leucogabbro	Medium	43	0	54	3	0	Holocrystalline, seriate, embayed cpx, poikilitic unzoned plag. Intergranular texture in places with cpx.
8-P-4	Leucogabbro	Medium	22	4	66	8	0	Holocrystalline, seriate, 120° dihedral angles + kinked twinning in plag, resorbed cpx + amph.
4-P-1	Anorthosite	Medium	4	0	89	1	6	Holocrystalline, med unzoned plag.
4-P-2	Leucogabbro	Coarse	10	35	42	3	10	Hypocrystalline, large amph in fine crystalline plag matrix with med zone plag crystals + vesiculated glass.
4-P-5	Leucogabbro	Medium	17	29	44	7	3	Layered, plag + cpx + opaque and amph + plag + opaque layers, euhedral to subhedral crystal, long axis aligned parallel to layers.
Mafic plutonic inclusions								
8-P-8	Amph gabbro	Medium	17	41	34	5	3	Seriate, anhedral crystals of amph with seriate plag and cpx.
8-P-10	Amph gabbro	Coarse	15	64	11	7	3	Seriate, coarse anhedral amph. in matrix of fine cpx and plag.
8-P-12	Cpx gabbro	Medium	63	12	12	7	6	Seriate, coarse anhedral amph. in matrix of fine cpx and plag.
Co-magmatic enclaves								
8-B-1	Basalt	Fine	19	2	21	4	54	Porphyritic with phenocrysts of relatively simply zoned plag, cpx and oxides, fluid contacts with host basaltic-andesite.
4-B-1	Basalt	Fine	18	4	23	4	51	Porphyritic with phenocrysts of relatively simply zoned plag, cpx and oxides, fluid contacts with host basaltic-andesite.

Amph Amphibole, *cpx* clinopyroxene, *plag* plagioclase, *gm* groundmass

^a Grain sizes: coarse > 5 mm, medium 1–5 mm, fine < 1 mm

Whole rock geochemistry of highly crystalline basaltic-andesite inclusions, co-magmatic enclaves and plutonic inclusions

The whole rock major and trace element composition for representative analysed plutonic inclusions and enclaves are listed in supplementary Table 1. Harker and Fenner diagrams for the most illustrative elements in the plutonic inclusion suite are shown in Fig. 8.

There is no appreciable difference in major element composition between the HCBA inclusions and their host basaltic-andesites. Both the HCBA inclusions and the 1994 and 1998 basaltic-andesites analysed in this study have 52–55 wt% SiO₂ and 2–4 wt% MgO. This range is in agreement with the published range for recent and historic high-K basaltic-andesite rocks from Merapi that show between 52 and 56 wt% SiO₂ and 2–4 wt% MgO, respectively (Gertisser and Keller 2003a, b). Slight variations in CaO, in turn, are a function of modal plagioclase

content. Analysed co-magmatic basaltic enclaves have a more restricted range and are mafic relative to the basaltic-andesite hosts with 49–52 wt% SiO₂ and 3–8 wt% MgO. The plutonic crystalline inclusions display a relatively broad range in SiO₂ (40–55 wt%) and MgO (3–11 %) with the mafic inclusions possessing MgO values of 9–11 wt%, whereas values recorded for the felsic inclusions give between 8 and 3 wt% MgO. Fe₂O₃, MgO and CaO contents decrease from mafic plutonic inclusions toward the felsic ones along broadly negative arrays when plotted against SiO₂ (Fig. 8). Positive trends are observed between SiO₂ and Na₂O, and K₂O (Fig. 8). P₂O₅ shows a positive and a negative array with increasing SiO₂ (Fig. 8). When plotting MgO as index of differentiation against, for example, TiO₂ and Al₂O₃, a compositional gap between the mafic plutonic inclusions and the other samples becomes apparent.

Whole rock REE data are presented in supplementary Table 1 and plotted on chondrite-normalised multi-element variation diagrams in Fig. 9. The co-magmatic basaltic

Table 2 Representative mineral analyses for plutonic inclusions, co-magmatic enclaves and amphibole megacrysts

Type	Plutonic inclusion			Basaltic enclaves			Megacrysts	
Sample	4-P-5	8-P-5	8-P-12	8-B-1	8-B-1	4-B-1	AM-108	AM-108
Crystal	A-1	A-2	A-1	A-1	A-2	A-1	A-4	A-7
a) Amphibole								
wt%								
SiO ₂	41.72	40.57	40.02	43.26	42.99	40.8	39.82	40.44
TiO ₂	2.54	2.42	1.73	2.2	2.41	2.18	1.95	1.87
Al ₂ O ₃	11.55	13.6	14.66	10.66	11.06	13.33	14.6	14.5
FeO*	14.94	12.74	12.59	12.76	12.5	13.17	10.59	10.72
MnO	0.42	0.20	0.23	0.39	0.45	0.19	0.18	0.17
MgO	11.91	12.78	12.9	13.98	13.71	13.07	14.37	14.23
CaO	11.21	12.04	11.89	11.13	11.16	11.48	12.41	12.49
Na ₂ O	2.56	2.60	2.20	2.54	2.44	2.44	2.28	2.24
K ₂ O	1.00	0.87	1.05	0.90	1.02	0.91	1.22	1.29
H ₂ O	2.03	2.04	2.04	2.06	2.06	2.05	2.05	2.06
Total	97.85	97.8	97.26	97.8	97.72	97.56	97.42	97.94
Structural formulae on the basis of 23 O								
Si	6.175	5.974	5.876	6.297	6.272	5.973	5.822	5.891
Al ^(iv)	1.825	2.026	2.124	1.703	1.728	2.027	2.178	2.109
Al ^(vi)	0.189	0.334	0.412	0.126	0.174	0.273	0.337	0.380
Ti	0.283	0.268	0.191	0.240	0.264	0.24	0.214	0.205
Cr	0	0	0	0	0	0	0	0
Fe ³⁺	0.593	0.452	0.765	0.74	0.657	0.81	0.648	0.547
Fe ²⁺	1.256	1.116	0.781	0.813	0.868	0.802	0.647	0.758
Mn	0.053	0.025	0.028	0.048	0.055	0.024	0.022	0.021
Mg	2.627	2.805	2.823	3.033	2.981	2.852	3.131	3.089
Ca	1.778	1.900	1.871	1.736	1.745	1.801	1.945	1.950
Na	0.734	0.741	0.626	0.716	0.69	0.692	0.646	0.632
K	0.189	0.162	0.197	0.168	0.189	0.170	0.228	0.240
Type	Plutonic inclusion			Basaltic enclaves				
Sample	8-P-1	8-P-4	8-P-12	8-P-10	8-B-1	8-B-1	4-B-1	4-B-1
Crystal	Px-2a	Px-1a	Px-1a	Px-1a	Px-1a	Px-2a	Px-2	Px-4
b) Pyroxene								
wt%								
SiO ₂	50.96	52.21	51.45	46.69	51.76	51.26	48.44	51.21
TiO ₂	0.46	0.38	0.48	1.16	0.44	0.41	0.79	0.37
Al ₂ O ₃	2.36	2.71	2.80	7.11	1.68	2.03	5.61	2.60
Cr ₂ O ₃	0.04	0.41	0.01	0.02	0.02	0.08	0.01	0.04
FeO*	8.94	4.31	8.58	8.23	8.26	8.22	9.63	8.23
MnO	0.43	0.07	0.44	0.22	0.59	0.57	0.28	0.43
MgO	14.57	15.70	14.80	12.46	15.02	14.54	12.95	15.07
CaO	21.14	23.61	21.04	23.31	20.97	21.12	21.78	21.16
Na ₂ O	0.52	0.23	0.37	0.31	0.35	0.40	0.37	0.33
Total	99.42	99.63	99.96	99.51	99.08	98.63	99.85	99.44

Table 2 continued

Type	Plutonic inclusion				Basaltic enclaves			
Sample	8-P-1	8-P-4	8-P-12	8-P-10	8-B-1	8-B-1	4-B-1	4-B-1
Crystal	Px-2a	Px-1a	Px-1a	Px-1a	Px-1a	Px-2a	Px-2	Px-4
Structural formulae on the basis of 6 O								
Si	1.696	1.738	1.712	1.554	1.723	1.706	1.612	1.704
Al ^(iv)	0.101	0.081	0.094	0.257	0.065	0.074	0.194	0.096
Al ^(vi)	0.003	0.037	0.028	0.055	0.009	0.016	0.052	0.017
Ti	0.012	0.010	0.012	0.029	0.011	0.010	0.020	0.009
Cr	0.001	0.008	0	0	0	0.002	0	0.001
Fe ³⁺	0.109	0.028	0.065	0.159	0.057	0.061	0.123	0.081
Fe ²⁺	0.170	0.105	0.201	0.098	0.201	0.197	0.177	0.175
Mn	0.006	0.001	0.006	0.003	0.008	0.008	0.004	0.006
Mg	0.361	0.389	0.367	0.309	0.372	0.361	0.321	0.374
Ca	0.377	0.421	0.375	0.416	0.374	0.377	0.388	0.377
Na	0.008	0.004	0.006	0.005	0.006	0.006	0.006	0.005
Type	Felsic plutonic inclusion				Mafic plutonic inclusion			
Sample	8-P-1	8-P-1	8-P-4	8-P-4	8-P-10	8-P-10	8-P-11	8-P-11
Crystal	P2core	P2rim	P2	P6	P1	P5	P2core	P2rim
c) Feldspar								
wt%								
SiO ₂	52.38	45.56	52.74	43.56	48.79	47.99	44.46	56.66
Al ₂ O ₃	29.88	33.87	28.27	34.54	31.88	32.64	35.10	26.65
FeO*	0.59	0.73	0.47	0.39	0.51	0.47	0.49	0.42
CaO	12.96	18.01	11.14	18.91	15.18	16.2	19.06	9.46
Na ₂ O	4.01	1.40	5.02	0.87	2.98	2.31	0.70	5.91
K ₂ O	0.29	0.04	0.39	0.04	1.78	0.145	0.02	0.49
BaO	0	0	0	0	0	0	0	0
Total	100.1	99.59	98.03	98.31	99.51	99.76	99.85	99.59
Or	2	0	2	0	1	1	0	3
Ab	35	12	44	8	26	20	6	52
An	63	88	54	92	73	79	94	46
Type	Basalt enclaves							
Sample	8-B-1	8-B-1	8-B-1	8-B-1	4-B-1	4-B-1	4-B-2	4-B-2
Crystal	GM-1	GM-2	GM-3	GM-4	P1core	P1rim	P1core	P1rim
c) Feldspar								
wt%								
SiO ₂	55.49	52.52	51.74	55.42	46.49	54.47	50.94	52.1
Al ₂ O ₃	27.68	28.75	29.9	27.92	33.32	27.72	30.13	29.29
FeO*	0.42	0.44	0.52	0.55	0.47	0.51	1.07	0.69
CaO	10.48	11.97	13.05	10.29	17.21	10.81	14.24	12.96
Na ₂ O	5.51	4.73	3.99	5.57	1.78	5.26	2.82	3.98
K ₂ O	0.43	0.35	0.26	0.43	0.08	0.38	0.78	0.54
BaO	0.09	0.05	0.05	0.05	0.01	0.05	0.07	0.07
Total	100.1	98.81	99.51	100.2	99.37	99.19	100.0	99.64
Or	2	2	1	2	0	2	5	3
Ab	48	41	35	48	16	46	25	15
An	50	57	63	49	84	52	70	62

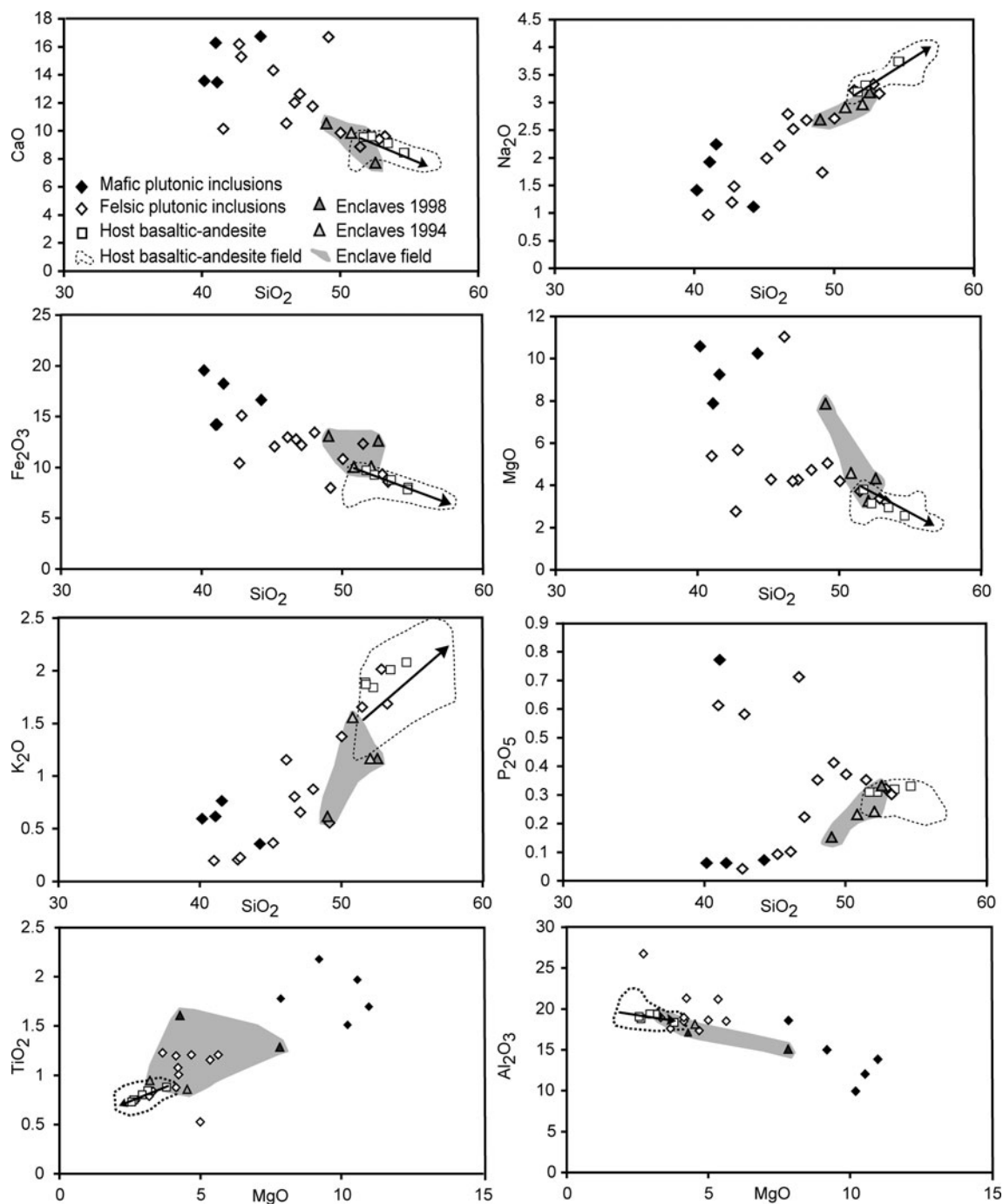


Fig. 8 Harker and Fenner diagrams for Merapi inclusions plotted relative to data fields for Merapi host rock values (from Gertisser and Keller 2003a, b). Host lavas and enclaves are highlighted by black

dashed lines and grey fields respectively. Arrows indicate fractionation trends from Gertisser and Keller (2003a, b)

enclaves have similar REE concentrations to Merapi basaltic-andesites and similarly possess elevated light REE (LREE, La-Sm) relative to chondrite and flat heavy REE (HREE) distribution (La_N/Lu_N : 2.5–5.2; Dy_N/Yb_N : 0.2–1.2). A positive Eu anomaly is seen in these enclaves, but a slight negative Eu anomaly is present in one sample (Fig. 9c). Many of the plutonic inclusions also display

patterns similar to Merapi host basaltic-andesites, especially for LREE (Fig. 9b, 1994 and some 1998 inclusions; La_N/Lu_N : 4.0–5.7). However, several samples (e.g. some of the 1998 plutonic inclusions; Fig. 9a) show moderate to marked depletion in LREE (La_N/Lu_N : 1.9–3.1) compared to Merapi basaltic-andesites (La_N/Lu_N : 2.6–6.4), and all samples have an enrichment in middle to HREE relative to

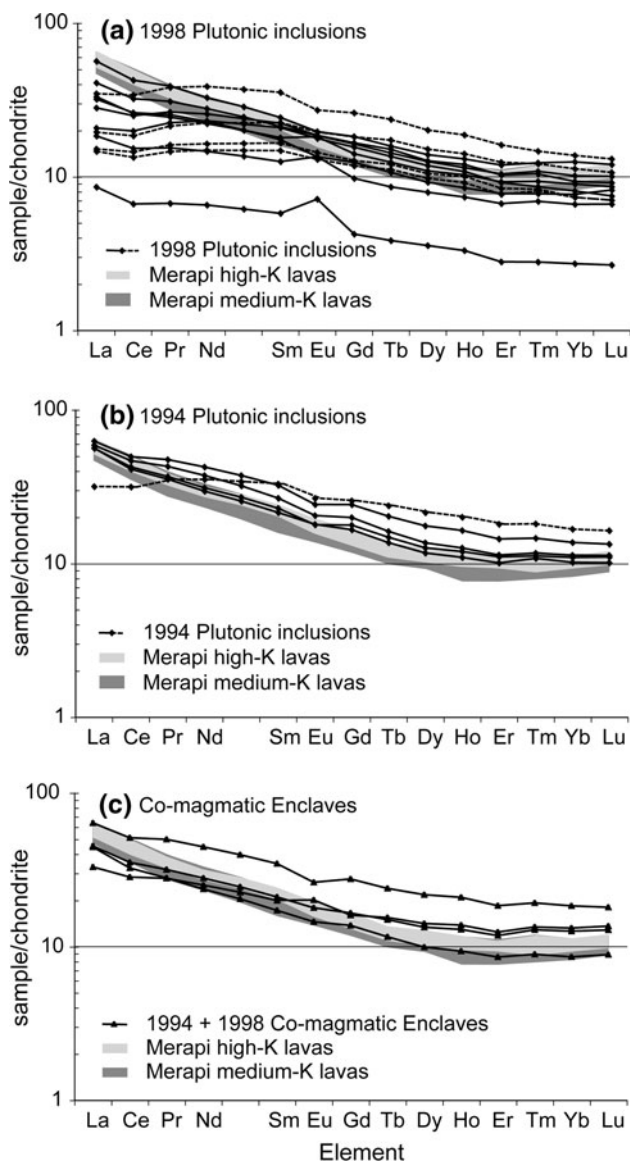


Fig. 9 Chondrite-normalised rare earth element diagram for Merapi plutonic inclusions, co-magmatic enclaves and Merapi High- and Medium-K lavas (after Gertisser and Keller 2003a). Dashed lines denote mafic plutonic inclusions, while the solid lines represent felsic inclusions. Chondrite data are from Sun and McDonough (1989). Pm was not analysed, the point is averaged between Nd and Sm

Merapi host lavas (Fig. 9), due to presence of titanite and several other accessory phases. Some plutonic inclusion samples exhibit a positive Eu anomaly, reflecting the accumulation of plagioclase. The inclusions from the 1994 deposits possess generally higher REE concentrations than samples from the 1998 deposits, particularly for LREE.

The Sr, Nd and Pb isotope data presented in this study are listed in supplementary Table 1 and plotted in Fig. 10. Isotope ratios for enclaves and plutonic crystalline inclusions fall within a range defined by published lava data for Merapi volcano (Gertisser and Keller 2003a). Only felsic

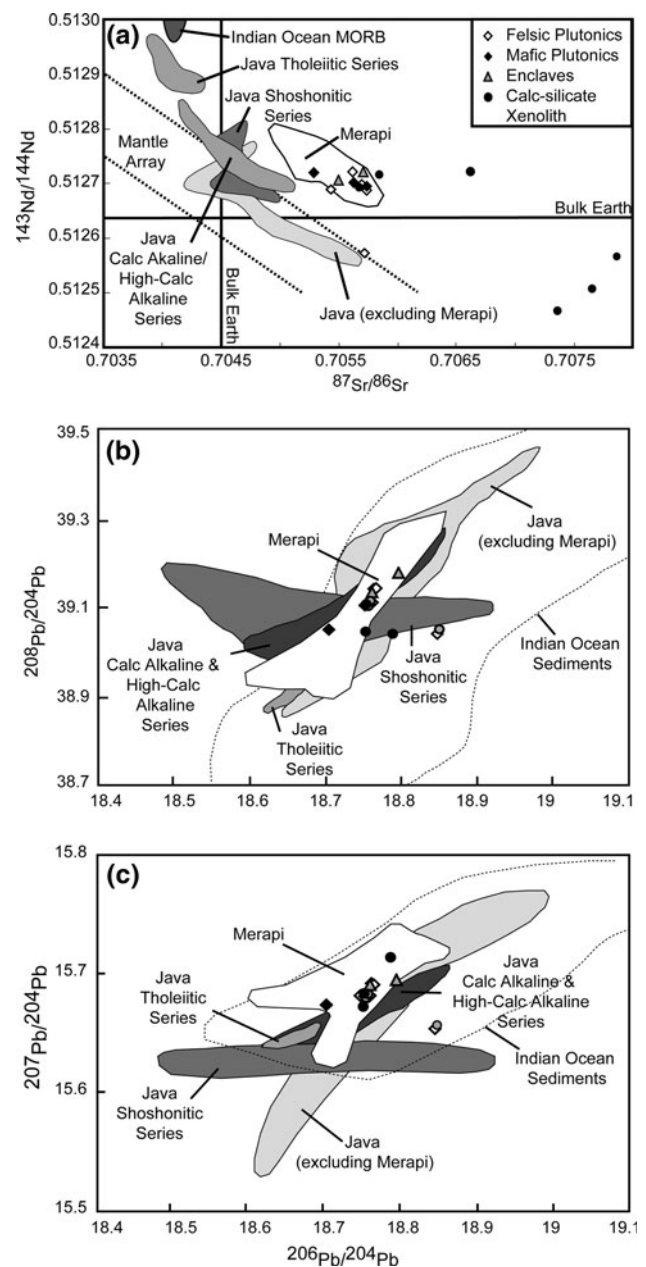


Fig. 10 a $^{143}\text{Nd}/^{144}\text{Nd}$ vs. $^{87}\text{Sr}/^{86}\text{Sr}$ diagram illustrating data from Merapi basaltic-andesite lavas, plutonic inclusions, enclaves and xenoliths relative to the Mantle array, Merapi lava compositions and data from other Javanese volcanoes (after Gertisser and Keller 2003a), b $^{208}\text{Pb}/^{204}\text{Pb}$ versus $^{206}\text{Pb}/^{204}\text{Pb}$ diagrams and c $^{207}\text{Pb}/^{204}\text{Pb}$ versus $^{206}\text{Pb}/^{204}\text{Pb}$ diagrams, both showing data from Merapi lavas, plutonic inclusions, enclaves and calc-silicate xenoliths relative data from other Javanese volcanoes, Indian Ocean MORB, Local upper crustal xenoliths and Indian Ocean sediment (after Gertisser and Keller 2003a)

plutonic inclusion 4-P-2 falls outside this range, with a much lower $^{143}\text{Nd}/^{144}\text{Nd}$ ratio relative to the other samples, but a similar Sr isotope ratio (Fig. 10a). Specifically, the co-magmatic basaltic enclaves give a narrow range from 0.70550 to 0.70571 for $^{87}\text{Sr}/^{86}\text{Sr}$ and from 0.51270 to

0.51272 for $^{143}\text{Nd}/^{144}\text{Nd}$, while the plutonic inclusions have a range for $^{87}\text{Sr}/^{86}\text{Sr}$ of 0.70529–0.70574 and of 0.51256–0.51272 for $^{143}\text{Nd}/^{144}\text{Nd}$. $^{206}\text{Pb}/^{204}\text{Pb}$ ratios for plutonic inclusions range from 18.71 to 18.75 and for co-magmatic basaltic enclaves from 18.76 to 18.80 (Fig. 10). $^{207}\text{Pb}/^{204}\text{Pb}$ ratios for plutonic inclusions and basaltic enclaves range from 15.65 to 15.69 and 15.69 to 15.70, respectively. The spread of $^{208}\text{Pb}/^{204}\text{Pb}$ ratios is relatively restricted, with plutonic inclusions and basaltic enclaves ranging from 39.04 to 39.14 and 39.14 to 39.18, respectively. The Pb data also overlap with the published range for Merapi host lavas (e.g. $^{208}\text{Pb}/^{204}\text{Pb} = 39.02\text{--}39.22$; Gertisser and Keller 2003a).

Discussion

Origin of inclusions and implications for the Merapi magma system

In order to use the geochemistry of the igneous inclusions as a tool to identify and interpret processes in the Merapi plumbing system and to establish its architecture, we must first determine that these inclusions are indeed from the Merapi magma system, or if material from the deep crust was incorporated into Merapi magmas by accident (i.e. xenolithic).

Highly crystalline basaltic-andesite (HCBA) inclusions

Although HCBA inclusions were analysed for major elements only, (4-P-9; Fig. 2a, b, supplementary Table 1), they are mineralogically and compositionally almost identical to their host basaltic-andesites (e.g. 4-A1). However, their strung out fluidal contacts support the concept of dynamic mixing and mingling processes acting in the Merapi plumbing system. These may come about through mixing of distinct basaltic-andesite batches or through recycling of semi-solidified crystal mushes from reservoir walls. This is consistent with evidence for reheating and recrystallisation at higher temperatures in the host basaltic-andesites, including reversely zoned plagioclase with dusty sieve-textured rims (e.g. Chadwick et al. 2007). Similar textures have been reported from many mingled and hybrid magmas and are thought to form by reheating above solidus temperature, followed by rapid recrystallisation to form more calcic rims (Tsuchiyama 1985; Nakamura and Shimakita 1996).

Co-magmatic basaltic enclaves

Basaltic enclaves in volcanic rocks are usually interpreted as products of mixing between two co-existing liquids (i.e. co-magmatic) (e.g., Bacon 1986; Eichelberger et al. 2000; Troll et al. 2004; Wiesmaier et al. 2011). Textural

relationships of the enclaves with their host rocks, such as lobate to elliptical shapes, chilled margins, fine grain size, acicular to elongate crystal groundmass and low degree of overall crystallinity, suggest relatively short interaction time of blobs of magma on contact with cooler host melt (see Coombs et al. 2002; Troll et al. 2004). Given the textural relationships (e.g. chilled contacts with the host basaltic-andesite), the enclaves analysed here are interpreted to indicate magma mixing as a result of mafic replenishments into the Merapi plumbing system.

This is consistent with pyroxene and plagioclase compositions from the enclaves that largely overlap with the reference data for the host basaltic-andesite pyroxenes (Figs. 5, 6). Normal zoning in the micro-feldspars is from bytownite cores (An_{70-90}) to labradorite to andesine rims with a groundmass crystal composition of An_{49-65} . This variation is probably best explained by changes in physical and chemical conditions during the formation of crystals at depth, for example, or during ascent (e.g. Beard and Borgia 1989; Housh and Luhr 1991; Sisson and Grove 1993; Panjasawatwong et al. 1995).

Major element compositions of the analysed basaltic enclaves vary from mafic basalt to within the basaltic-andesite field (Fig. 8), consistent with Merapi's evolutionary trends from basalt to basaltic-andesite (e.g. Gertisser and Keller 2003a, b). The REE patterns of the basaltic enclaves also overlap in part with the host basaltic-andesite patterns (Fig. 9), and the radiogenic isotope ratios of the enclaves consistently plot within the Merapi basaltic-andesite field (Fig. 10). As the enclaves are isotopically similar to the host basaltic-andesites, with slight variations in major and REE composition, they provide a useful record of the evolution from hydrous, mafic basalt to amphibole-poor basaltic-andesite.

Plutonic crystalline inclusions

Numerous geochemical studies of subduction zone volcanoes have identified plutonic igneous inclusions in lavas, inferred to reflect the residues of differentiation processes that have operated on the magmas of these arcs (e.g. Beard 1986; Fichaut et al. 1989; Beard and Borgia 1989; Heliker 1995; Costa et al. 2002). However, the bulk rock compositions of plutonic rocks are likely to vary significantly from the liquid composition from which they have originally formed by crystal accumulation and/or melt migration (e.g. McBirney 1995).

Many of the plutonic inclusions analysed here possess clear petrographic evidence for crystal accumulation, such as uniformly coarse crystal sizes, alignment of minerals, modal mineral layering and mono-mineralogic bands. Polygonal crystal boundaries in two of the samples indicate prolonged periods of high temperature sub-solidus

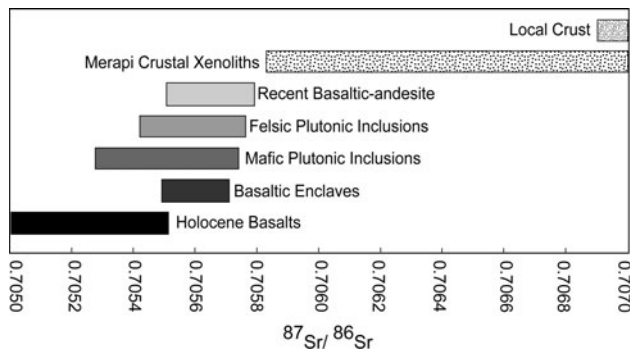


Fig. 11 Sr isotope variation diagram for inclusions plotted relative to recent Merapi basaltic-andesite lavas and Holocene basalts (from Gertisser and Keller 2003a). The data display a stepwise progression to more radiogenic isotopes from mafic to felsic inclusions (i.e. with degree of differentiation) and an overlap for the mafic inclusions with Holocene basalts is observed

conditions (c.f. Holness et al. 2007b). Zoned and embayed crystals occur at times and may indicate disequilibrium with percolating melts (Holness et al. 2007a). Thus, major trace element and REE trends observed in the plutonic inclusion whole rock geochemistry must be interpreted with respect to their formation. Like the basaltic enclaves, pyroxene and plagioclase compositions from the plutonic inclusions largely plot within the reference field for Merapi basaltic-andesite pyroxenes (Figs. 5, 6, 7), with the exception of a few slightly more calcic clinopyroxenes present. In contrast, the plutonic inclusions possess a relatively large spread in plagioclase compositions, extending up to An₉₅. This highly calcic feldspar may be a function of increased H₂O contents in a crystalline mush (c.f. Lundstrom and Tepley 2006), which is supported by the presence of significant amounts of amphibole in many of the inclusions (Figs. 10, 11).

Mineral accumulation relative to Merapi basaltic-andesites is also reflected by the whole rock variability in Al₂O₃, FeO, TiO₂, P₂O₅, K₂O and SiO₂. This corresponds to variations in the modal abundances of amphibole, plagioclase, apatite and Fe–Ti oxides, with a degree of scatter in the data consistent with selective mineral enrichment due to plutonic processes. Fe₂O₃, MgO, CaO and TiO₂ contents are generally high in mafic plutonic inclusions, while these are poor in K₂O and Na₂O, reflecting a high abundance of pyroxene and amphibole (Fig. 8). The whole rock compositions of many samples are broadly consistent with binary mixtures of pyroxene and plagioclase, or pyroxene and amphibole, in line with the high modal percentages of these three minerals.

However, the plutonic inclusions possess Ca/Na values ranging from compositions similar to Merapi basaltic-andesite (2–3; from Gertisser and Keller 2003a) to much higher values (2.75–17). This variation may come from a number of factors, but chiefly from fractionation/accumulation of plagioclase and/or apatite and/or from crustal assimilation of, for example, limestone. Interaction with

country rocks is not supported by the isotope data of these mafic inclusions, whereas P₂O₅ shows scattered arrays with increasing SiO₂ and decreasing MgO (Fig. 8). The majority of the inclusions possess also significantly lower (<0.2 wt%) or significantly higher (>0.5 wt%) P₂O₅ than the host basaltic-andesite and these trends can be quantified with either adding or subtracting about 40 % of the modal apatite component of a basaltic-andesite lava, respectively. Plutonic inclusions with low P₂O₅ contents (Fig. 8; <0.2 wt%) do not contain significant amounts of apatite, potentially indicating a loss of enriched melt prior to solidification and subsequent entrainment in Merapi basaltic-andesite. This has been reported for similar plutonic inclusions in, for example, San Pedro volcano in Chile (Costa et al. 2002). These authors proposed that P₂O₅ variability was due to a combination of processes, involving liquid loss from a crystal pile before or after apatite crystallisation. Alternatively, the enrichment in apatite may be due to interaction with carbonate country rock or melts, as apatite is a common mineral in contact metamorphosed calc-silicates. Calc-silicate inclusions have been observed as a xenolith type in one of the felsic plutonic inclusions, but are rare and hence cumulate processes are likely to dominate. This is in line with many of the REE patterns of the plutonic inclusions that overlap with those of the host basaltic-andesite (Fig. 9). However, there is a moderate to marked depletion in LREE relative to Merapi host lavas in several of the samples from the 1998 eruption, which agrees with high plagioclase and low pyroxene modal proportions in these specific samples. Loss of interstitial liquid rich in REE (see above) potentially amplified this effect. Enrichment in middle REE (Fig. 9), particularly in the samples from the 1994 eruption, is likely to be a reflection of a dominance in amphibole (hornblende), clinopyroxene and titanite in these samples. Flat to positive Eu anomalies in the plutonic inclusions reflect plagioclase accumulation, also potentially amplified by loss of interstitial liquid rich in REE, that is, with a negative Eu signature.

Sr, Nd and Pb isotope compositions of plutonic inclusions largely fall within the range of published data for Merapi volcano (e.g. Gertisser and Keller 2003a and references therein), highlighting their cognate nature. Sr isotope ratios obtained for representative samples of plutonic inclusions show a stepwise progression from lower radiogenic Sr values for the mafic inclusions to mildly higher radiogenic values for the felsic inclusion (Fig. 11; supplementary table 1). Moreover, there is an apparent overlap between Holocene Merapi basalts with a medium K content (Medium-K series) and the mafic plutonic inclusions in particular (Fig. 11). Given this overlap with the older magma series, they likely formed from solidification of older magmas in the Merapi system and were subsequently re-mobilised. Recent whole rock lavas, in turn, show an

elevated range that trends toward the higher values of the crustal samples (cf. Chadwick et al. 2007).

Amphibole megacrysts

The amphibole megacrysts share strong geochemical (Table 2) and petrographic links with the plutonic inclusions (e.g. 8-P-3, Fig. 4b) and together with the observed disequilibrium textures (Fig. 4) indicate that they were likely not crystallised directly from the host Merapi lavas, but rather from a deeper and more hydrous composition within the plumbing system of the volcano. The fine-grained reaction rims on the amphibole megacrysts and on a percentage of the smaller amphibole crystals present in Merapi basaltic-andesite are likely to be formed by volatile loss from the magma during ascent or because of reheating (Devine et al. 1998; Rutherford and Devine 2003; Davidson et al. 2007). These reaction rims are not always well developed or can be absent in the smallest amphibole phenocrysts contained within some Merapi pumice ejecta, implying a mixture of real phenocrysts and antecrystic amphibole megacrysts (e.g. Gertisser et al. 2011). However, the large disequilibrium rims present in the amphibole megacrysts likely form due to slow ascent outside the amphibole stability field (i.e. at pressures less than ~ 150 MPa). As there is extensive petrographic evidence of reheating in the Merapi magma system, such as mafic mixing, mingling textures and plagioclase sieve textures, reheating of the magma may also in part have produced the amphibole reaction textures. Reheating textures are not always easy to distinguish from pure ascent/decompression-induced reactions (cf. Barclay et al. 1998, Blundy and Cashmann 2001; Rutherford and Devine 2003), but likely both phenomena are represented.

Depth structure of the Merapi plumbing system

The petrography and geochemistry, and particularly the isotope data of the igneous inclusions, underline that they are petrogenetically linked to the Merapi magma system, that is, they are for most parts cognate (i.e. ‘antelithic’). It is therefore possible to use the intrinsic conditions of their formation to describe stages (or levels) of the Merapi magma supply system that are potentially not recorded in the host lavas. Geobarometric calculations using minerals from these inclusions could thus provide a significant step to constrain the physical characteristics of the Merapi plumbing system.

There is a paucity of suitable geobarometers for garnet-free mafic to intermediate rocks in the literature and the geobarometric calculations presented here therefore offer a first-order approximation only. Gertisser (2001) calculated a range of crystallisation temperatures from 920 to 1,050 °C for the Merapi basaltic-andesite lavas from co-existing oxides and thus an average temperature of

1,000 °C has been used for our geobarometric models. Calculations for temperatures across the full range defined by Gertisser (2001) show generally limited fluctuation in resulting pressures estimates.

A link between clinopyroxene crystal chemistry and pressure of crystallization has been established by several authors (Dal Negro et al. 1982, 1984, 1989; Manoli and Molin 1988; Nimis 1995, 1999; Nimis and Ulmer 1998). According to Nimis and Ulmer (1998), and Nimis (1995, 1999), pressure can be expressed as linear function of the crystallographic unit cell volume and the corresponding volume available for the M_1 site and thus relating stoichiometric composition to crystallisation pressure of clinopyroxene. The standard error on prediction of pressure crystallization values is generally around ± 140 MPa (Nimis 1999). Recent work on more hydrous and higher SiO_2 experimental compositions has highlighted inherent weaknesses in this model, which appears to slightly underestimate crystallization pressures for more evolved and/or more hydrous systems (Putirka et al. 2003), but should provide a perfectly reasonable first approximation for the Merapi system.

The Nimis (1999) barometer was applied to electron microprobe analyses of pyroxenes from basaltic-andesites and the variety of inclusions in the Merapi lavas. A range of pyroxene crystallisation pressures from ~ 100 to 1,300 MPa was obtained (Fig. 12), with a concentration of values between 400 and 700 MPa. Results for host

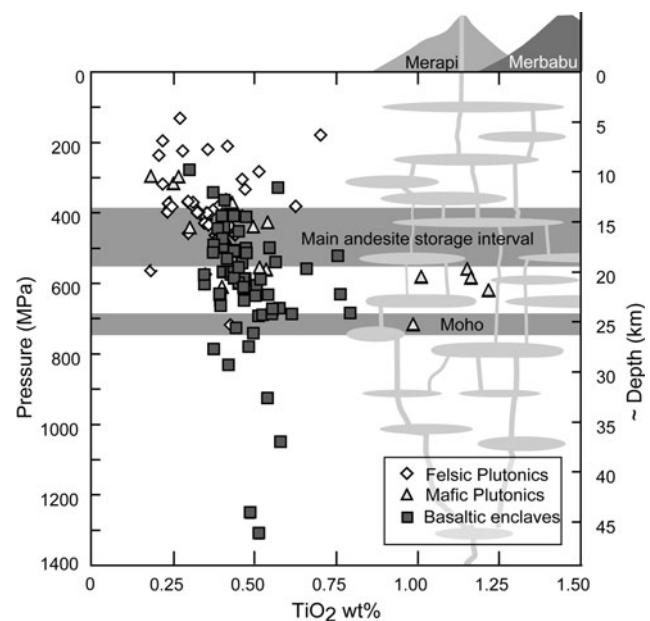


Fig. 12 Results of pyroxene barometry after Nimis (1999), plotted relative to TiO_2 wt% content of crystals and approximate depth of crystallisation. Main zone of basaltic-andesite crystallisation (from Gertisser 2001) shown for comparison. Uncertainties of the barometry results are ± 140 MPa. The data indicates a wide spread in crystallisation pressures for the different inclusions

basaltic-andesites range from 200 to 900 MPa with the bulk of pyroxene crystals having formed between 400 and 500 MPa. This agrees with earlier findings by Gertisser (2001). Assuming reasonable densities for the Merapi edifice ($\sim 2.6 \text{ g/cm}^3$), the Javan crust (2.8 g/cm^3), and the upper mantle (3.3 g/cm^3), the bulk of pyroxenes in the basaltic-andesites must have crystallised in mid- to deep crustal reservoirs (12–18 km; Fig. 12). The most extreme pyroxenes from the inclusions in turn crystallised as shallow as $\sim 3 \text{ km}$ beneath the summit to as deep as $\sim 45 \text{ km}$ below it, but with the bulk of crystallisation occurring in a semi-diffuse zone in the mid-crust (Fig. 12). Pyroxenes in felsic plutonic inclusions have crystallisation pressures between 65 and 720 MPa (2–25 km). The lower pressure results are generally confined to the rims of these crystals and reflect storage in very shallow parts of the plumbing system, and we observe that the majority of crystallisation occurred at pressures of between 300 and 400 MPa ($\sim 10\text{--}15 \text{ km}$). Pyroxenes in mafic plutonic inclusions have similar crystallisation pressures to the felsic inclusions, but with values between 300 and 720 MPa. Co-magmatic basaltic enclave pyroxenes have the deepest crystallisation pressures, from $\sim 300 \text{ MPa}$ to 1,300 MPa, consistent with magma storage extending well into the upper mantle ($\sim 45 \text{ km}$ depth; Fig. 12).

Although merely a first-order approximation, the results from geobarometry on lavas and igneous inclusions from Merapi suggest a crystallisation record that spans almost the entire thickness of the crust and into the upper mantle. As these inclusions are taken to represent cognate compositions or more coarsely crystalline fragments of parental Merapi magmas, the spread of pressure results suggests the presence of magma storage reservoirs at multiple depths throughout the crust and into the lithospheric mantle beneath the volcano, where crystallisation and magma evolution are taking place in numerous small reservoirs and pockets.

A comparison of the crystallisation pressures obtained in this study with seismic data from Ratdompurbo and Popinet (2000) shows a link between seismic anomalies in the shallow crust beneath Merapi and the lower crystallisation pressures of ~ 300 to 400 MPa obtained from a small number of felsic plutonic inclusions. However, this is in contrast to more-recent geophysical studies that were unable to locate a shallow magma reservoir like that proposed by Ratdompurbo and Popinet (2000). Neither gravity, GPS, tilt nor seismic data could find unequivocal support for the presence of a larger shallow magma reservoir within or just below the Merapi edifice (Tiede et al. 2005; Westerhaus et al. 1998; Beauducel and Cornet 1999; Wasserman et al. 1998; Maercklin et al. 2000; Wegler and Lühr 2001; Müller et al. 2002; Müller and Haak 2004). Given the low crystallisation pressures obtained from felsic inclusions in this study, late crystallization may occur in

many small ephemeral magma pockets in the shallow crust prior to eruption and/or on ascent in the conduit, consistent with frequent crystalline basaltic-andesite schlieren and domains in the erupted lavas. However, using the full barometric data range of pyroxene, the bulk of magma storage feeding volcanism at Merapi must occur at deeper levels, specifically in the mid-crust ($\sim 12\text{--}18 \text{ km}$). Amphibole megacrysts share characteristics with the amphibole compositions in the mafic plutonic inclusions and are thus likely also from a deeper and more hydrous reservoir, which is located in the mid- to lower crust beneath Merapi (Peters et al. 2011). The intense reaction textures of the amphibole megacrysts are mainly from chemical disequilibrium reaction of the megacrysts with the more silicic basaltic-andesite magmas and must not be confused with purely decompression related amphibole instability (e.g. Rutherford and Hill 1993; Blundy and Cashmann 2001; Barclay and Carmichael 2004), which has been noted in smaller amphibole crystals (true phenocrysts) in Merapi lavas too (Gertisser et al. 2011).

Although the deeper structure beneath Merapi and Central Java remains poorly defined (Koulakov et al. 2007; Wagner et al. 2007), the heterogeneity in the geochemical, petrological and geobarometric data detailed above implies that it is unlikely that this deeper storage is hosting one single magma body. The system, likely, consists of a plexus of potentially ephemeral partly solidified, crystal-rich, semi-molten and locally entirely molten magma pockets with remnants of former crust inbetween the pockets. Multiple chambered systems have been proposed for comparable subduction zone volcanoes (e.g. Price et al. 2005; Jaxybulatov et al. 2011; Dahren et al. 2012). A large and complex, multi-chambered, plumbing system has considerable long-term implications for hazard assessment and monitoring at Merapi as the volcano may be a relatively small surface expression of a much larger magmatic system that is present and further developing at depth.

Implications

The petrology and geochemistry of magmatic enclaves and plutonic inclusions is crucial for understanding the petrogenesis and structure of the Merapi plumbing system as a whole. The geochemistry and petrology of plutonic crystalline inclusions, co-magmatic enclaves and HCBA inclusions provides evidence for a complex open-system feeding Merapi volcanism with mixing, mingling, crystallisation, crystal accumulation, crustal contamination and periodical recharges, all being frequent processes at work. This record of magmatic evolution is only poorly preserved in the relatively homogenised host basaltic-andesite lavas.

In more detail, the co-magmatic enclaves are evidence of the intrusion of mafic magmas into more fractionated

crystalline magmas at high levels within the plumbing system. This, in likely combination with underplating of a hot mafic magma beneath more felsic reservoirs, would result in frequent remobilisation of highly crystalline residual mushes via reheating and partial melting. This would make it possible for the magmas to mingle, resulting in the formation of mafic enclaves in the basaltic-andesite host magmas. Most probably, a number of shallow magma pockets beneath Merapi volcano exist as a large shallow chamber cannot be detected, but the upper crust beneath Merapi is nevertheless marked by up to 30 % fluid (magma) present (Wagner et al. 2007; Koulakov et al. 2007). This is best reconciled by the notion of a number of smaller chambers and pockets, especially in the top few kilometres of the crust beneath the volcano. Each of these is sizeable enough to produce a slightly different solidification and evolutionary stage of the hosted magmas, but sufficiently small to escape detection by tomographic means (e.g. <5 km × 5 km; Wagner et al. 2007; Chadwick 2008; Troll et al. 2012b), thus giving rise to the sheer variety of plutonic and crystalline inclusions observed. This situation appears somewhat analogous to the plumbing system at, for example, present-day Krakatau (Dahren et al. 2012; Jaxybulatov et al. 2011) or Ruapehu (Price et al. 2005, 2007, 2012) and may be characteristic of this volcano-type. Further support for magma mixing and mingling is found in the presence of HCBA inclusions and in the plagioclase sieve textures in the basaltic-andesite host, indicating multiple reheating events. Reheating is then a probable cause for increased convection, which is thought to help initiate eruptions; a number of eruptive events at arc volcanoes have been documented, associated with mixing that was followed by eruption within a relatively short period of time (e.g. Sparks et al. 1977; Pallister et al. 1992; Martin et al. 2008).

The plutonic crystalline inclusions and HCBA inclusions thus support the idea of recycling of crystalline material within the magmatic system of Merapi; a process that has been widely identified in other arc magmas as well (e.g. Tepley et al. 2000; Turner et al. 2003; Dungan and Davidson 2004). Given the long-lived nature of Merapi volcanism (<170,000 years, Gertisser et al. 2012), it is sensible to conclude that a significant mass of crystalline material has accumulated in the crust below the volcano, and the HCBA inclusions and amphibole megacrysts demonstrate that this material is regularly recycled into ascending magmas. Given the mid- to lower crustal level of main magma storage at Merapi (main amphibole and pyroxene crystallisation) indicated by the combined geobarometric and geophysical studies (e.g. Wagner et al. 2007; Chadwick 2008), it is essential for the deep seismic activity of this volcano to be monitored to better constrain the relationships between replenishment and eruptions and

to improve timely warning of impending activity. In conjunction with geophysical data, there is also strong evidence for the presence of multiple pockets and reservoirs filled with semi-molten crystalline mush in the crust directly beneath Merapi, and this also has implications for magma chemistry and hazard assessment. For example, the CO₂ budget of the magma is likely affected by assimilation of mid- to shallow level carbonate crust, which will become significant at depth above approximately 10 km (c.f. Deegan et al. 2010; Troll et al. 2012a, b). Lastly, the presence of mafic to ultramafic lithologies argues for recycling of deep plutonic roots of the magmatic system (e.g., Heliker 1995; Dungan and Davidson 2004; Reubi and Blundy 2008; Davidson et al. 2007). This has significant implications for geochemical mass balance assessments of the Merapi magma system, as partial assimilation of its own plutonic roots and various crustal components will overprint primary geochemical signatures that are important for source studies (Debaillie et al. 2006; Dungan and Davidson 2004; Reubi and Blundy 2008). Mass balance models for the Merapi system must thus take account of the heterogeneities of the Merapi magma system in order to produce meaningful results.

Acknowledgments We are grateful to M. Gardner and M. Mahjum for help during sample collection. The authors would also like to acknowledge T. Leeper for help with the isotope analysis. Discussion with J. Gamble, B. Lühr, E. M. Jolis and D. Wagner was much appreciated. We also acknowledge generous financial support from the EC Marie Curie mobility scheme, the Danish National Research Foundation, the Mineralogical Society of Great Britain and Ireland and the Swedish Science Foundation (VR).

References

- Abdurachman EK, Bourdier JL, Voight B (2000) Nuées ardentes of November 22 1994 at Merapi Volcano, Indonesia. *J Volcanol Geotherm Res* 100:345–361
- Abratis M, Schmincke H-U, Hansteen TH (2002) Composition and evolution of submarine volcanic rocks from the central and western Canary Islands. *Int J Earth Sc* 91:562–582
- Andreastuti SD, Alloway BV, Smith IM (2000) A detailed tephrostratigraphic framework at Merapi Volcano, Central Java, Indonesia: implications for eruption predictions and hazard assessment. *J Volcanol Geotherm Res* 100:51–67
- Annen C, Blundy JD, Sparks RSJ (2006) The genesis of intermediate and silicic magmas in deep crustal hot zones. *J Petrol* 47(3): 505–539
- Bacon CR (1986) Magmatic inclusions in silicic and intermediate volcanic rocks. *J Geophys Res* 91:6091–6112
- Bahar I (1984) Contribution à la connaissance du volcanisme Indonésien: le Merapi (Centre Java); cadre structural, pétrologie, géochimie et implications volcanologiques. Dissertation, Université des Sciences et Techniques du Languedoc
- Baker J, Peate DW, Waight T, Meyzen C (2004) Pb isotopic analysis of standards and samples using a 207Pb–204Pb double spike and thallium to correct for mass bias with a double focusing MC-ICP-MS. *Chem Geol* 211:275–303

- Barclay J, Carmichael ISE (2004) A hornblende basalt from Western Mexico: water-saturated phase relation constrains a pressure-temperature window of eruptibility. *J Petrol* 45(3):485–506
- Barclay J, Rutherford MJ, Carroll MR (1998) Experimental phase equilibria constraints on pre-eruptive storage conditions of the Soufrière Hills magma. *Geophys Res Lett* 25:3437–3440
- Beard JS (1986) Characteristic mineralogy of arc-related cumulate gabbros: implications for the tectonic setting of gabbroic plutons and for andesite genesis. *Geology* 14:848–851
- Beard JS, Borgia A (1989) Temporal variation of mineralogy and petrology in cognate gabbroic enclaves at Arenal volcano, Costa Rica. *Contrib Mineral Petrol* 103:110–122
- Beauducel F, Cornet FH (1999) Collection and three-dimensional modeling of GPS and tilt data at Merapi Volcano, Java. *J Geophys Res* 104:725–736
- Bird P (2003) An updated digital model of plate boundaries. *Geochem Geophys Geosyst* 4(3):1027. doi:10.1029/2001GC000252
- Blundy J, Cashmann K (2001) Ascent-driven crystallization of dacite magmas at Mount St Helens, 1980–1986. *Contrib Mineral Petrol* 140:631–650
- Bodinier J-L, Guiraud M, Fabries J, Dostal J, Dupuy C (1987) Petrogenesis of layered pyroxenites from the Lherz, Freychinede and Prades ultramafic bodies (Ariege, French Pyrenees). *Geochim Cosmochim Acta* 51:279–290
- Bowen NL (1928) The evolution of the igneous rocks. Princeton University Press, Princeton, pp 1–132
- Burt RM, Brown SJA, Cole JW, Shelley D, Waight TE (1998) Glass-bearing plutonic fragments from ignimbrites of the Okataina caldera complex, Taupo Volcanic Zone, New Zealand: remnants of a partially molten intrusion associated with preceding eruptions. *J Volcanol Geotherm Res* 84:209–237
- Campbell IH (1978) Some problems with cumulus theory. *Lithos* 11:311–323
- Camus G, Gourgaud A, Mossand-Berthommier PC, Vincent PM (2000) Merapi (Central Java, Indonesia): an outline of the structural and magmatological evolution, with a special emphasis to the major pyroclastic events. *J Volcanol Geotherm Res* 100:139–163
- Chadwick JP (2008) Magma crust interaction in volcanic systems: case studies from Merapi Volcano, Indonesia, Taupo Volcanic Zone, New Zealand, and Slieve Gullion, N.Ireland. PhD thesis, Trinity College Dublin, Ireland
- Chadwick JP, Troll VR, Giniere C, Morgan D, Gertisser R, Waight TE, Davidson JP (2007) Carbonate assimilation at Merapi volcano, Java Indonesia: insights from crystal isotope stratigraphy. *J Petrol* 48(9):1793–1812
- Coombs ML, Eichelberger JC, Rutherford MJ (2002) Experimental and textural constraints on mafic enclave formation in volcanic rocks. *J Volcanol Geotherm Res* 119:125–144
- Costa F, Dungan M, Singer B (2002) Hornblende- and phlogopite-bearing gabbroic xenoliths from Volcán San Pedro (368S), Chilean Andes: evidence for melt and fluid migration and reactions in subduction-related plutons. *J Petrol* 43:219–241
- Curry JR, Shor GG, Raitt RW, Henry M (1977) Seismic refraction and reflection studies of crustal structure of the Eastern Sunda and Western Banda arcs. *J Geophys Res* 82:2479–2489
- Dahren B, Troll VR, Andersson UB, Chadwick JP, Gardner MF, Jaxybulatov K, Koulikov I (2012) Magma plumbing beneath Anak Krakatau volcano, Indonesia: evidence for multiple magma storage regions. *Contrib Mineral Petrol* 163:631–651
- Dal Negro A, Carbonin S, Molin GM, Cundari A, Piccirillo EM (1982) Intracrystalline cation distribution in natural clinopyroxene of tholeiitic, transitional and alkaline basaltic rocks. In: Saxena SK (ed) *Advances in physical geochemistry*, vol 2. Springer, New York, pp 117–150
- Dal Negro A, Carbonin S, Domeneghetti C, Molin GM, Cundari A, Piccirillo EM (1984) Crystal chemistry and evolution of the clinopyroxenes in a suite of high-pressure ultramafic rocks from the Newer Volcanics of Victoria, Australia. *Contrib Mineral Petrol* 86:221–229
- Dal Negro A, Molin GM, Salviulo G, Secco L, Cundari A, Piccirillo EM (1989) Crystal chemistry of pyroxene and its petrogenetic significance: a new approach. In: Boriani A, Bonafede M, Piccardo GB, Vai GB (eds) *The lithosphere in Italy: advances of earth science research*. Acc Naz Lincei, Atti Convegno Lincei 80:271–295
- Davidson JP, Tepley FJ (1997) Recharge in volcanic systems: evidence from isotope profiles of phenocrysts. *Science* 275:826–829
- Davidson JP, Turner S, Handley H, McPherson C, Dosseto A (2007) Amphibole “sponge” in arc crust? *Geology* 35(9):787–790
- Davies JH, Stevenson DJ (1992) A physical model of source region of subduction zone volcanics. *J Geophys Res* 97:2027–2037
- de Genevraye P, Samuel L (1972) Geology of the Kendeng Zone (Central & East Java). Proceedings, first annual convention, Indonesian Petroleum Association, pp 17–30
- Debaille V, Doucelance R, Weis D, Schiano P (2006) Multistage mixing in subduction zones: application to Merapi volcano, (Java Island, Sunda arc). *Geochim Cosmochim Acta* 70:723–741
- Deegan FM, Troll VR, Freda C, Misiti V, Chadwick JP, McLeod CL, Davidson JP (2010) Magma-carbonate interaction processes and associated CO₂ Release at Merapi Volcano, Indonesia: insights from experimental petrology. *J Petrol* 51(5):1027–1051
- Deegan FM, Troll VR, Freda C, Misiti V, Chadwick JP (2011) Fast and furious: crustal CO₂ release at Merapi volcano, Indonesia. *Geol Today* 27(2):63–64
- Deer WA, Howie RA, Zussman J (1992) Rock forming minerals. Longman, London
- del Marmol MA (1989) The petrology and geochemistry of Merapi Volcano, Central Java Indonesia. Dissertation, Johns Hopkins University, Baltimore
- DePaolo DJ (1981) Trace element and isotopic effects of combined wallrock assimilation and fractional crystallization. *Earth Planet Sci Lett* 53:189–202
- Devine JD, Rutherford MJ, Gardner JE (1998) Petrologic determination of ascent rates for the 1995–1997 Soufrière Hills Volcano andesitic magma. *Geophys Res Lett* 25:3673–3676
- Dungan MA, Davidson JP (2004) Partial assimilative recycling of the mafic plutonic roots of arc volcanoes: an example from the Chilean Andes. *Geology* 32(9):773–776
- Eichelberger JC, Chertkoff DG, Dreher ST, Nye CJ (2000) Magmas in collision: rethinking chemical zonation in silicic magmas. *Geology* 28:603–606
- Fichaut M, Marcelot G, Clocchiatti R (1989) Magmatology of Mt. Pelée (Martinique, F.W.I.). II: petrology of gabbroic and dioritic cumulates. *J Volcanol Geotherm Res* 38:171–187
- Garcia MO, Jacobson SS (1979) Crystal clots, amphibole fractionation and the evolution of calc-alkaline magmas. *Contrib Mineral Petrol* 69:319–327
- Gertisser R (2001) Gunung Merapi (Java, Indonesien): Eruptionsgeschichte und magmatische Evolution eines Hochrisiko-Vulkans. Dissertation: Universität Freiburg
- Gertisser R, Keller J (2003a) Trace element and Sr, Nd, Pb and O isotope variations in medium-K and high-K volcanic rocks from Merapi Volcano, Central Java, Indonesia: evidence for the involvement of subducted sediments in Sunda Arc Magma Genesis. *J Petrol* 44:457–489
- Gertisser R, Keller J (2003b) Temporal variations in magma composition at Merapi Volcano (Central Java, Indonesia): magmatic cycles during the past 2000 years of explosive activity. *J Volcanol Geotherm Res* 123:1–23
- Gertisser R, Charbonnier SJ, Troll VR, Keller J, Preece K, Chadwick JP, Barclay J, Herd RA (2011) Merapi (Java, Indonesia): anatomy of a killer volcano. *Geol Today* 27:57–62

- Gertisser R, Charbonnier SJ, Keller J, Queidelleur X (2012) The geological evolution of Merapi volcano, Central Java, Indonesia. *Bull Volcanol* 74:1213–1233
- Gill JB (1981) *Orogenic andesites and plate tectonics*. Springer, New York
- Grove TL, Kinzler RJ (1986) Petrogenesis of Andesites. *Ann Rev Earth Planet Sci* 14:417–454
- Grove TL, Kinzler RJ, Baker MB, Donnelly-Nolan JM, Leshner CE (1988) Assimilation of granite by basaltic magma at Burnt Lava flow, Medicine Lake volcano, northern California: decoupling of heat and mass transfer. *Contrib Mineral Petrol* 99:320–343
- Hamilton W (1979) *Tectonics of the Indonesian region 1979*. United States Geol Surv Prof Paper 1078:1–345
- Hammer JE, Cashman KV, Voight B (2000) Magmatic processes revealed by textural and compositional trends in Merapi dome lavas. *J Volcanol Geotherm Res* 100:165–192
- Heliker C (1995) Inclusions in Mount St. Helens dacite erupted from 1980 through 1983. *J Volcanol Geotherm Res* 66:115–135
- Hidayat D, Voight B, Langston C, Ratdomopurbopurbo A, Ebeling C (2000) Broadband seismic experiment at Merapi Volcano, Java, Indonesia: very-long-period pulses embedded in multiphase earthquakes. *J Volcanol Geotherm Res* 100:215–231
- Hildreth W, Moorbath S (1988) Crustal contributions to arc magmatism in the Andes of Chile. *Contrib Mineral Petrol* 98:455–489
- Holness MB, Hallworth MA, Woods A, Sides E (2007a) Infiltration Metasomatism of Cumulates by Intrusive Magma Replenishments: the Wavy Horizon, Isle of Rum, Scotland. *J Petrol* 48(3):563–587
- Holness MB, Anderson AT, Martin VM, MacLennan J, Passmore E, Schwindinger K (2007b) Textures in partially solidified crystalline nodules: a window into the pore structure of slowly cooled mafic intrusions. *J Petrol* 48(7):1243–1264
- Housh TB, Luhr JF (1991) Plagioclase-melt equilibria in hydrous system. *Am Mineral* 76:477–492
- Hunter RH (1987) Textural equilibrium in layered igneous rocks. In: Parsons I (ed) *Origins of igneous layering*. D. Reidel Publishing Company, Boston, pp 473–503
- Irving AJ (1974) Megacrysts from the Newer basalts and the other basaltic rocks of southeastern Austr. *Geol Soc Am Bull* 85:1503–1514
- Irving AJ, Frey FA (1984) Trace element abundances in megacrysts and their host basalts: constraints on partition coefficients and megacryst genesis. *Geochim Cosmochim Acta* 48:1201–1221
- Itoh H, Takahama J, Takahashi M, Miyamoto K (2000) Hazard estimation of the possible pyroclastic flow disasters using numerical simulation related to the 1994 activity at Merapi volcano. *J Volcanol Geotherm Res* 100:503–516
- Jarrard RD (1986) Relations among subduction parameters. *Rev Geophys* 24:217–284
- Jaxybulatov K, Koulakov I, Ibs-von Seht M, Klinge K, Reichert C, Dahren B, Troll VR (2011) Evidence for high fluid/melt content beneath Krakatau volcano (Indonesia) from local earthquake tomography. *J Volcanol Geotherm Res* 206:96–105
- Koulakov I, Bohm M, Asch G, Luehr B-G, Manzanares A, Brotopuspito KS, Fauzi N, Purbawinata MA, Puspito NT, Ratdomopurbo A, Kopp H, Rabbel W, Shevkunova E (2007) P- and S-velocity structure of the crust and the upper mantle beneath Central Java from local tomography inversion. *J Geophys Res* 112:B08310. doi:10.1029/2006JB004712
- Le Maitre RW (1989) *A classification of igneous rocks and glossary of terms: recommendations of the international union of geological sciences, subcommission on the systematics of igneous rocks*. Blackwell, Oxford
- Leake BE, Woolley AR, Arps CES, Birch WD, Gilbert MC, Grice JD et al (1997) Nomenclature of amphiboles: report of the subcommittee on amphiboles of the International Mineralogical Association, commission on new minerals and mineral names. *Am Mineral* 82:1019–1037
- Luais B, Telouk P, Albarède F (1997) Precise and accurate neodymium isotopic measurements by plasma-source mass spectrometry. *Geochim Cosmochim Acta* 61:4847–4854
- Lundstrom CC, Tepley FJ (2006) Investigating the origin of anorthitic plagioclase through a combination of experiments and natural observations. *J Volcanol Geotherm Res* 157:202–221
- Maercklin N, Riedel C, Rabbel W, Wegler U, Lühr B-G, Zschau J (2000) Structural investigation of Mt. Merapi by an active seismic experiment. *Mitteil/Deutschen Geophysik Gesell* 4:13–16
- Manoli S, Molin GM (1988) Crystallographic procedures in the study of experimental rocks: X-ray single-crystal structure refinement of C2/c clinopyroxene from Lunar 74275 high-pressure experimental basalt. *Mineral Petrol* 39:87–200
- Martin VM, Morgan DJ, Jerram DA, Caddick MJ, Prior DJ, Davidson JP (2008) Bang! Month-scale eruption triggering at Santorini volcano. *Sci* 321:1178
- McBirney AR (1995) Mechanisms of differentiation in the Skaergaard Intrusion. *J Geol Soc Lond* 152:421–435
- Morimoto N (1988) Nomenclature of pyroxenes. *Am Mineral* 73:1123–1133
- Müller A, Haak V (2004) 3-D modeling of the deep electrical conductivity of Merapi Volcano (Central Java): integrating magnetotellurics, induction vectors and the effects of steep topography. *J Volcanol Geotherm Res* 138:205–222
- Müller M, Hördt A, Neubauer FM (2002) Internal structure of Mount Merapi, Indonesia, derived from long-offset transient electromagnetic data. *J Geophys Res* 107:2–14
- Nakamura M, Shimakita S (1996) Partial dissolution kinetics of plagioclase: implication for magma mixing time scale and origin of melt inclusions. *EOS Trans Am Geophys Un* 77(46):F841
- Newhall CG, Bronto S, Alloway B, Banks NG, Bahar I, del Marmol MA, Hadisantono RD, Holcomb RT, McGeehin J, Miksic JN, Rubin M, Sayudi SD, Sukhyar R, Andreastuti S, Tilling RI, Torley R, Trimble D, Wirakusumah AD (2000) 10,000 Years of explosive eruptions of Merapi Volcano, Central Java: archeological and modern implications. *J Volcanol Geotherm Res* 100:9–50
- Nimis P (1995) A clinopyroxene geobarometer for basaltic systems based on crystal-structure modeling. *Contrib Mineral Petrol* 121:115–125
- Nimis P (1999) Clinopyroxene geobarometry of magmatic rocks. Part 2. Structural geobarometers for basic to acid, tholeiitic and midly alkaline magmatic systems. *Contrib Mineral Petrol* 135:62–74
- Nimis P, Ulmer P (1998) Clinopyroxene geobarometry of magmatic rocks. Part 1. An expanded structural geobarometer for anhydrous and hydrous, basic and ultrabasic systems. *Contrib Mineral Petrol* 133:314–327
- Pallister JS, Hoblitt RP, Reyes AG (1992) A basalt trigger for the 1991 eruptions of Pinatubo Volcano. *Nature* 356:426–428
- Panjasawatwong Y, Danyushevsky LV, Crawford AJ, Harris KL (1995) An experimental study of the effects of melt composition on plagioclase-melt equilibria at 5 and 10 kbar: implications for the origin of magmatic high-An plagioclase. *Contrib Mineral Petrol* 118:420–432
- Peters STM, Chadwick JP, Troll VR (2011) Amphibole antecrysts in deposits of Merapi volcano, Indonesia: a plutonic phase in extrusive magmas. *Goldschmidt supplement. Mineral Mag* 75:1627
- Pietranik A, Waight TE (2008) Processes and sources during late Variscan Dioritic-Tonalitic magmatism: insights from plagioclase chemistry (Gęsiniec Intrusion, NE Bohemian Massif, Poland). *J Petrol* 49:1619–1645
- Price RC, Gamble JA, Smith IEM, Stewart RB, Eggins S, Wright IC (2005) An integrated model for the temporal evolution of

- andesites and rhyolites and crustal development in New Zealand's North Island. *J Volcanol Geotherm Res* 140:1–24
- Price RC, George R, Gamble JA, Turner S, Smith IEM, Cook C, Hobden B, Dosseto A (2007) U-Th-Ra fractionation during crustal-level andesite formation at Ruapehu volcano, New Zealand. *Chem Geol* 244(3–4):437–451
- Price RC, Turner S, Cook C, Hobden B, Smith IEM, Gamble JA, Möbis A (2010) Crustal and mantle influences and U-Th-Ra disequilibrium in andesitic lavas of Ngauruhoe Volcano, New Zealand. *Chem Geol* 277(3–4):355–373
- Price RC, Gamble JA, Smith IEM, Maas R, Waight TE, Stewart RB, Woodhead J (2012) The anatomy of an andesitic volcano: a time-stratigraphic study of andesite petrogenesis and crustal evolution at Ruapehu Volcano, New Zealand. *J Petrol* 53:2139–2189
- Putirka KD, Mikaelian H, Ryerson F, Shaw H (2003) New clinopyroxene-liquid thermobarometers for mafic, evolved, and volatile-bearing lava compositions, with applications to lavas from Tibet and the Snake River Plain, Idaho. *Am Mineral* 88:1542–1554
- Ratdomopurbo A, Poupinet G (2000) An overview of the seismicity of Merapi volcano (Java, Indonesia), 1983–1994. *J Volcanol Geotherm Res* 100:193–214
- Renzulli A, Santi P (1997) Sub-volcanic crystallization at Stromboli (Aeolian Islands, southern Italy) preceding the Sciara del Fuoco sector collapse: evidence from monzonite lithic-suite. *Bull Volcanol* 59:10–20
- Reubi O, Blundy J (2008) Assimilation of plutonic roots, formation of high-K 'exotic' melt inclusions and genesis of andesitic magmas at Volcán de Colima, Mexico. *J Petrol* 49:2221–2243
- Rogers G, Hawkesworth CJ (1989) A geochemical traverse across the North Chilean Andes: evidence for crust generation from the mantle wedge. *Earth Plan Sci Lett* 91:271–285
- Rutherford MJ, Devine JD (2003) Magmatic conditions and magma ascent as indicated by hornblende phase equilibria and reactions in the 1995–2002 Soufrière Hills magma. *J Petrol* 44:1433–1453
- Rutherford MJ, Hill PM (1993) Magma ascent rates from amphibole breakdown: an experimental study applied to the 1980–1986 Mount St. Helens eruptions. *J Geophys Res* 98:19667–19685
- Schwarzkopf LM, Schmincke H-U, Troll VR (2001) Pseudotachylite on impact marks of block surfaces in block-and ash flows at Merapi volcano, Central Java, Indonesia. *Int J Earth Sci* 90:769–775
- Schwarzkopf LM, Schmincke H-U, Cronin SJ (2005) A conceptual model for block-and-ash flow basal avalanche transport and deposition, based on deposit architecture of 1998 and 1994 Merapi flows. *J Volcanol Geotherm Res* 139:117–134
- Simkin T, Siebert L (1994) *Volcanoes of the world*. Geoscience Press Inc., Tuscon
- Sisson TW, Bronto S (1998) Evidence for pressure-release melting beneath magmatic arcs from basalt at Galunggung, Indonesia. *Nature* 391:883–886
- Sisson TW, Grove TL (1993) Experimental investigations of the role of H₂O in calc-alkaline differentiation and subduction zone magmatism. *Contrib Mineral Petrol* 113:143–166
- Siswowardjyo S, Suryo I, Yokoyama I (1995) Magma eruption rates of Merapi volcano, Central Java, Indonesia during one century (1880–1992). *Bull Volcanol* 57:111–116
- Smyth HR, Hall R, Hamilton J, Kinny P (2005) East Java: Cenozoic basins, volcanoes and ancient basement. In: *Proceedings, Indonesian Petroleum Association. Thirtieth Annual Convention & Exhibition*, pp 251–266
- Sparks RSJ, Sigurdsson H, Wilson L (1977) Magma mixing—mechanism for triggering acid explosive eruptions. *Nature* 267:315–318
- Streckeisen A (1976) To each plutonic rock its proper name. *Earth Sci Rev* 12:1–33
- Sun SS, McDonough WF (1989) Chemical and isotopic systematics of oceanic basalts: implications for mantle composition and processes. In: Saunders AD, Norry MJ (eds) *Magmatism in the Ocean Basins*. Geological Society, London, Special Publications 42:313–345
- Surono, Jousset P, Pallister J, Boichu M, Buongiorno M, Budisantoso A, Costa F, Andreastuti S, Prata F, Schneider D, Clarisse L, Humaida H, Sumarti S, Bignami C, Griswold J, Cam S, Oppenheimer C (2012) The 2010 explosive eruption of Javas Merapi volcano a 100-year event. *J Volcanol Res*. doi:10.1016/j.jvolgeores.2012.06.018
- Tepley FJ, Davidson JP, Tilling RI, Arth JG (2000) Magma mixing, recharge and eruption histories recorded in plagioclase phenocrysts from El Chichon volcano, Mexico. *J Petrol* 41:397–1411
- Thouret J-C, Lavigne F, Kelfoun K, Bronto S (2000) Toward a revised hazard assessment at Merapi volcano, Central Java. *J Volcanol Geotherm Res* 100:479–502
- Tiede C, Camacho AG, Gerstenecker C, Fernández J, Suyanto I (2005). Modeling the density at Merapi volcano area, Indonesia, via the inverse gravimetric problem. *Geochim Geophys Geosyst* 6:Q09011. doi:10.1029/2005GC000986
- Tregoning P, Brunner FK, Bock Y, Pundotowo SSO, McCaffrey R, Genrich JF, Calais E, Rais J, Subaraya C (1994) First geodetic measurement of convergence across the Java Trench. *Geophys Res Lett* 21:2135–2138
- Troll VR, Donaldson CH, Emeleus CH (2004) Pre-eruptive magma mixing in ash-flow deposits of the Tertiary Rum Igneous Centre, Scotland. *Contrib Mineral Petrol* 147:722–739
- Troll VR, Hilton DR, Jolis EM, Chadwick JP, Blythe LS, Deegan FM, Schwarzkopf LM, Zimmer M (2012a) Crustal CO₂ liberation during the 2006 eruption and earthquake events at Merapi volcano, Indonesia. *Geophys Res Lett* 39:L11302. doi:10.1029/2012GL051307
- Troll VR, Deegan FM, Jolis EM, Harris C, Chadwick JP, Gertisser R, Schwarzkopf LM, Borisova A, Bindeman IN, Sumarti S, Preece K (2012b) Magmatic differentiation processes at Merapi volcano: inclusion petrology and oxygen isotopes. *J Volcanol Geotherm Res* (in revision)
- Tsuchiyama A (1985) Dissolution kinetics of plagioclase in the melt of the system diopside–albite–anorthite, and origin of dusty plagioclase in andesite. *Contrib Mineral Petrol* 89:1–16
- Turner SP, Platt JP, George RMM, Kelley SP, Pearson DG, Nowell GM (1999) Magmatism associated with orogenic collapse of the Betic–Alboran domain, SE Spain. *J Petrol* 40:1011–1036
- Turner S, George R, Jerram D, Carpenter N, Hawkesworth C (2003) Some case studies of plagioclase growth and residence times in island arc lavas from the Lesser Antilles and Tonga, and a model to reconcile apparently disparate age information. *Earth Planet Sci Lett* 214:279–294
- Untung M, Sato Y (1978) Gravity and geological studies in Java, Indonesia. *Geol Survey of Indonesia and Geological Survey of Japan, Special Publication* 6:207
- van Bemmelen RW (1949) *The geology of Indonesia, vol 1 A., General Geol.* The Hague, Government Printing Office, The Netherlands
- Voight B, Constantine EK, Siswowardjyo S, Torley R (2000) Historical eruptions of Merapi Volcano, Central Java, Indonesia, 1768–1998. *J Volcanol Geotherm Res* 100:69–138
- Wager LR, Brown GM (1968) *Layered igneous rocks*. W.H. Freeman, San Francisco
- Wagner D, Koulakov I, Rabbel W, Luehr B-G, Wittwer A, Kopp H, Bohm M, Asch G, The MERAMEX Scientists (2007) Joint inversion of active and passive seismic data in Central Java. *Geophys J Intern* 170(2):923–932
- Waight TE, Baker JA, Peate DW (2002) Sr isotope ratio measurements by double focusing MC-ICPMS: techniques, observations and pitfalls. *Intern J Mass Spectrom* 221:229–244

- Wassermann J, Ohrnberger M, Scherbaum F (1998) Continuous measurements at Merapi Volcano (Java, Indonesia) using a network of small-scale seismograph arrays; In: J Zschau & M Westerhaus (ed), Decade-Volcanoes under Investigation, Dt Geophys Ges 3:81–82
- Wegler U, Lühr B-G (2001) Scattering behaviour at Merapi volcano (Java) revealed from an active seismic experiment. *Geophys J Intern* 145:579–592
- Westerhaus M, Rebscher D, Welle W, Pfaff A, Körner A, Nandaka M (1998) Deformation measurements at the flanks of Merapi Volcano. In: J Zschau & M Westerhaus (ed) Decade-Volcanoes under Investigation, Dt. Geophys Ges 3:93–100
- Wiesmaier S, Deegan FM, Troll VR, Carracedo JC, Chadwick JP, Chew JM (2011) Magma mixing in the 1100 AD Montaña Reventada composite lava flow, Tenerife, Canary Islands: interaction between rift zone and central volcano plumbing systems. *Contrib Mineral Petrol* 162:651–669